Feedbacks between Air Pollution and Weather, Part 1: Effects on Weather

P.A. Makar[1], W. Gong[1], J. Milbrandt[2], C. Hogrefe[3], Y. Zhang[4], G. Curci[5], R. Žabkar[6,7], U. Im[8,*], A. Balzarini[9], R. Baró[10], R. Bianconi[11], P. Cheung[1], R. Forkel[12], S. Gravel[13], M. Hirtl[14], L. Honzak[7], A. Hou[1], P. Jiménez-Guerrero[11], M. Langer[14], M.D. Moran[1], B. Pabla[1], J.L. Pérez[15], G. Pirovano[9], R. San José[15], P. Tuccella[16], J. Werhahn[12], J. Zhang[1], S. Galmarini[8]

[1]*Air-Quality Research Division, Environment Canada, Toronto, Canada*
[2]*Meteorological Research Division, Environment Canada, Montreal, Canada*
[3]*Atmospheric Modeling and Analysis Division, Environmental Protection Agency, Research Triangle Park, USA*
[4]*Department of Marine, Earth and Atmospheric Sciences, North Carolina State University, Raleigh, USA*
[5]*University of L'Aquila, L'Aquila, Italy*
[6]*University of Ljubljana, Ljubljana, Slovenia*
[7]*Center of Excellence SPACE-SI, Ljubljana, Slovenia*
[8]*Joint Research Centre, European Commission, Ispra, Italy*[9]*RSE, Milano, Italy*
[10]*University Murcia, MAR-UMU, Spain*
[11]*Enviroware (www.enviroware.com), Milan, Italy*
[12]*Karlsruhe Inst. of Technology, IMK-IFU, Garmisch-Partenkirchen*
[13]*Air-Quality Research Division, Environment Canada, Montreal, Canada*
[14]*ZAMG, Vienna, Austria*
[15]*Technical Univ. of Madrid, ESMG-UPM, Spain*
[16]*University L'Aquila, CETEMPS, L'Aquila, Italy*
[*]*(now at) Aarhus University, Department of Environmental Science, Roskilde, Denmark*

Corresponding author telephone/ fax and email: 1-416-739-4692 / 1-416-739-4288, paul.makar@ec.gc.ca

For submission to *Atmospheric Environment Special Issue on Phase 2 of the Air-Quality Model Evaluation International Initiative, May 27, 2014.*

Abstract

The meteorological predictions of fully coupled air-quality models running in "feedback" versus "no-feedback" simulations were compared against each other and observations as part of Phase 2 of the Air Quality Model Evaluation International Initiative. In the "no-feedback" mode, the aerosol direct and indirect effects were disabled, with the models reverting to either climatologies of aerosol properties, or a no-aerosol weather simulation. In the "feedback" mode, the model-generated aerosols were allowed to modify the radiative transfer and/or cloud formation parameterizations of the respective models. Annual simulations with and without feedbacks were conducted on domains over North America for the years 2006 and 2010, and over Europe for the year 2010.

The incorporation of feedbacks was found to result in systematic changes to forecast predictions of meteorological variables, both in time and space, with the largest impacts occurring in the summer and near large sources of pollution. Models incorporating only the aerosol direct effect predicted feedback-induced reductions in temperature, surface downward and upward shortwave radiation, precipitation and PBL height, and increased upward shortwave radiation, in both Europe and North America. The feedback response of models incorporating both the aerosol direct and indirect effects varied across models, suggesting the details of implementation of the indirect effect have a large impact on model results, and hence should be a focus for future research. The feedback response of models incorporating both direct and indirect effects was also consistently larger in magnitude to that of models incorporating the direct effect alone, implying that the indirect effect may be the dominant process. Comparisons across modelling platforms suggested that direct and indirect effect feedbacks may often act in competition: the sign of residual changes associated with feedbacks often changed between those models incorporating the direct effect alone versus those incorporating both feedback processes.

Model comparisons to observations for no-feedback and feedback implementations of the same model showed that differences in performance between models were larger than the performance changes associated with implementing feedbacks within a given model. However, feedback implementation was shown to result in improved forecasts of meteorological parameters such as the 2m surface temperature and precipitation. These findings suggest that meteorological forecasts may be improved through the use of fully coupled feedback models, or through incorporation of improved climatologies of aerosol properties, the latter designed to include spatial, temporal and aerosol size and/or speciation variations.

Introduction

This work examines the effects of air pollution on forecasts of weather, through the use of fully coupled air pollution / weather forecast models. A companion paper to this work (Makar *et al*, 2014) explores the

effects of feedbacks from air pollution on simulated atmospheric chemistry. Both studies were undertaken as part of Phase 2 of the Air Quality Model Evaluation International Initiative (AQMEII-2).

AQMEII-2 builds on the work begun under the first phase (AQMEII), an intercomparison of air pollution forecast models wherein most participating air pollution models were "off-line", that is to say, they required as input meteorological files from a weather forecast or climate model. Emissions inputs for these models as well as boundary conditions were harmonized, and the models were compared to air-quality observations using sophisticated statistical tools, for annual simulations of air quality for the year 2006 (Galmarini *et al*, 2012a,b; Solazzo *et al*.2012, a,b), for both Europe (EU) and North America (NA).

A more recent development in the modelling of the atmosphere for synoptic forecast timescales is the "on-line" air quality model, in which both chemistry and weather forecasts are created in the same modelling framework (e.g. Grell *et al*., 2005; Zhang, 2008; Moran *et al*., 2010; and cf. Baklanov *et al*., 2014 for a recent review of these models). Further description of the models specifically employed here and references for the construction of this first generation of feedback models appears in the Methodology section, and Table 1). On-line models reduce the computational overhead associated with the transfer of large meteorological input files into computer memory, and have the potential to reduce errors associated with interpolation between meteorological and air quality model grid projections. These models have the added advantage of allowing the possibility of incorporating feedbacks between air pollution and meteorology. These are known as "fully coupled" on-line models, as distinct from on-line models in which the chemical processes make use of meteorological information, without a reverse communication in which chemistry is allowed to alter the meteorology. Feedbacks are incorporated into global and regional climate models as a requirement for accurate climate prediction (cf. Forster *et al,* 2007), and the role of aerosols in accurate modelling of the atmosphere on climatological timescales has long been recognized (c.f. IPCC, 2007). However, climate models, because of the long time periods used for their simulations, the associated computational limitations, and the need to resolve the atmosphere of the entire Earth, usually do not employ atmospheric chemical processes with the same degree of sophistication as is

found in regional air-quality models. The role of aerosols in the radiative balance of the atmosphere via the radiative properties of the aerosols themselves (aerosol direct effect) or via the aerosols role in acting as cloud condensation nuclei (aerosol indirect effect) is key to climate model prediction accuracy, but remains a considerable source of uncertainty in model predictions (IPCC, 2007). Conversely, most meteorological models used to forecast weather on synoptic or shorter timescales use climatologies or simplified parameterizations of aerosol properties, in order to represent the aerosol direct and indirect effects. The cross-comparison fully coupled regional air-quality models is thus of interest to the scientific community, in order to better understand the role of feedback processes on the short time scales associated with weather forecasts, and to identify commonalities and differences between forecasts from different modelling platforms. The latter provides a means by which to identify model parameterizations requiring improvement. The models examined here are the first generation to include fully coupled weather/air-quality processes in a regional forecasting context, and this is the first attempt to quantify and cross-compare the impacts of direct and indirect effect aerosol feedbacks using these models.

In Phase 2 of AQMEII, on-line fully coupled regional models using harmonized emissions and chemical boundary conditions were inter-compared and evaluated against observations of air-quality and meteorology, for North American (NA) and European (EU) domains, for the years 2006 and 2010 (Im *et al*, 2014a,b, Yahya et al., 2014a, b; Campbell et al., 2014; Wang et al., 2014a, Brunner et al, 2014, Makar et al, this issue). Here, we focus on the specific issue of the extent to which feedback processes may influence weather forecasts, in order to attempt to address the following questions:

(1) Does the incorporation of feedbacks in on-line models result in systematic changes to their predicted meteorology?

(2) Do the changes vary in time and space?

(3) To what extent does the incorporation of feedbacks improve or worsen model results, compared to observations?

In Part 2 (Makar et al, 2014), we examine the effects of feedbacks on the model's chemical predictions. Here, we examine the effects of feedbacks on the models' meteorological predictions, with a focus on the common year for both domains, 2010.

Methodology

Table 1 provides details and references for the participating models' version numbers, cloud parameterizations, aerosol size representation and microphysics algorithms, meteorological initial and boundary conditions, land-surface models, planetary boundary layer schemes, radiative transfer schemes, gas-phase chemistry mechanisms, and the time period and model variables available for comparisons. Table 1 also provides details on the methodology used to allow the feedback models' aerosols to participate in radiative transfer calculations (aerosol direct effect), and in the formation of clouds as cloud condensation nuclei, which in turn may change the radiative and other properties of the simulated clouds (aerosol indirect effect). Ideally, the study of the impact of feedbacks on coupled model simulations would make use of two versions of each air-quality model, one in which the feedback mechanisms have been disabled, and the other with enabled feedback mechanisms. However, not all of the participating modelling groups in AQMEII-2 had the computational resources to carry out both non-feedback and feedback simulations, nor were all groups able to simulate both direct and indirect effect feedbacks. For the North American AQMEII simulations, only the group contributing the GEM-MACH model (Moran *et al*, 2010), modified here for both aerosol direct and indirect feedbacks, was able to simulate both of the years 2006 and 2010. The WRF-CMAQ model was used to generate direct-effect-only feedback simulations for 2006 and 2010, but no-feedback simulations were only generated for summer periods of each year. The WRF-CHEM model with a configuration for both direct and indirect effects was used for feedback simulations of both years, but no-feedback simulations were only available for this model for a one-month period and are discussed elsewhere (Wang et al., 2014b). However, simulations of weather using the equivalent WRF model in the absence of feedbacks were used to generate meteorological simulations (*de facto* without feedbacks due to the lack of chemistry in WRF). These simulations could

then be used for comparison to the meteorological output of the WRF-CHEM feedback simulations. For the EU AQMEII simulations, three WRF-CHEM simulations were compared for the year 2010: a version 3.4.1 no-feedback simulation in which all aerosol interactions with meteorology were disabled, a version 3.4.1 direct-effect-only simulation, and a version 3.4.0 simulation incorporating both direct and indirect effects. For the combined direct + indirect effect WRF-CHEM3.4.0 simulation, a WRF-only simulation was carried out to determine the feedback impacts on meteorology. The simulations thus comprise the best currently available model simulations for evaluating the effects of feedbacks – the choice of modelling platforms was not arbitrary, but dictated by the computational resources of the contributing research groups.

The underlying meteorological models may have parameterizations to represent aerosol effects, and the extent to which the parameterizations are used and their construction differs between the models. A "no-feedback" simulation is therefore not necessarily a "no aerosol" simulation. GEM-MACH's no-feedback mode includes parameterizations for the aerosol direct and indirect effect (the former using latitudinally varying aerosol optical properties and the latter a simple function of supersaturation, see Table 1). The WRF "no-feedback" implementations used here in the WRF-CHEM and WRF-CMAQ models have no direct effect parameterizations (aerosols treated as zero concentration), and a constant cloud droplet number of 250 cm^{-3} was used in place of a cloud condensation nucleus parameterization (Forkel *et al*, 2012). Differences between the models' response to feedbacks are thus also with respect to these pre-existing parameterizations or simplifications, and differences between these approaches may influence the variation in the models' response to feedbacks.

All models made use of their native meteorological driving analyses or nudging procedures. Under the AQMEII-2 protocol, the simulations were conducted in a stepped fashion. A meteorological spin-up period (the length of which was up to the individual participants, usually 12 to 24 hours) during which only meteorological processes, and no feedbacks, were used to bring the model's meteorology to a quasi-steady state with regards to cloud processes. This was followed by a 48 hour simulation of meteorology

and chemistry (either with or without feedbacks). In the subsequent staggered step, a second meteorology-only spin-up simulation began 12 to 24 hours before the end of the previous chemistry simulation. Upon reaching the time corresponding to the end of the previous simulation, the models would make use of that simulation's final chemical concentrations, continuing the process forward, with no-feedback or feedback simulations, for the next 48 hours. Most of the models used a data-assimilated meteorological analysis as the meteorological initial conditions for each of the staggered forecasts. As a result of this staggered-step procedure, the meteorological portions of the forecasts were not allowed to "drift" too far from meteorological objective analyses during the course of the simulations – the differences shown in this paper and Part 2 (Makar et al., 2014) are thus the net effect of feedbacks that occur over a sequence of 48 hour simulations, with the chemical concentrations generated by the two simulations being the single ongoing connecting factor between the paired simulations. The WRF-CMAQ model was run continuously for both 2006 and 2010 with low-strength nudging applied throughout the duration of the simulation (Hogrefe *et al*., 2014, this issue). Sensitivity simulations presented in Hogrefe *et al*. (2014) showed that nudging helped to improve model performance for 2m temperature while only slightly reducing the strength of the WRF-CMAQ simulated direct feedback effect. The use of native analyses or nudging procedures and the overlapping 48 hour forecasts thus imply the results shown here are of the highest relevance to synoptic forecasting time-scales, while providing valuable information for climatological modelling.

The horizontal resolutions of the models varied: GEM-MACH used 15 km horizontal, WRF-CHEM, 36 km, and WRF-CMAQ 12 km. The EU WRF-CHEM simulations employed a common horizontal resolution of 23 km. Further details on the models and their components may be found in Table 1, and further description of the models are provided in Campbell *et al* (2014), and Im et al (2014a,b)). The models used in the comparisons performed here were limited to those which had complete or partial no-feedback and feedback simulations for the AQMEII-2 model years; the full suite of AQMEII -2 models and comparisons to observations are also described in Im et al, (2014a,b).

The model simulations occurred on the "native" grid projection for each model, but were interpolated for cross-comparison purposes to common AQMEII latitude-longitude grids with a resolution of 0.25 degrees for the NA or EU domains, respectively. For the NA simulations, the native model grids overlapped this target grid to different degrees, so a common "mask" incorporating the union of all model projections on the common grid was employed. For the EU simulations, the different versions of WRF-CHEM were operated on the same native grid, though comparisons carried out here were conducted using the AQMEII European grid.

Feedback and non-feedback simulations were compared to each other in two ways. First, at every hour of simulation, the spatial variation between feedback and non-feedback model values on the AQMEII grids were compared using the statistical measures described in Table 2. This comparison allowed the identification of seasonal trends in the spatial impact of feedbacks, as well as particular time periods when these impacts were the strongest. Second, the model values at each gridpoint were compared across time (for the entire simulated year and for shorter time periods), allowing the creation of spatial maps of the impact of feedbacks on the common simulation variables. These maps help identify the regions where feedbacks have the largest effect on the simulation outcome. A comprehensive evaluation of all AQMEII-2 fully coupled models against meteorological observations occurs elsewhere (Brunner *et al*, 2014), while here we carry out that comparison with a subset of models, and focus on identifying the main impacts of the feedbacks on the forecasted meteorology.

1. Comparison of Model Simulations by Time Series

1.1 Temperature

Figure 1 shows the time series of the mean differences (a,b,c) and correlation coefficients (d,e,f) for each model for the year 2010 for the North American (NA) domain models. Both the WRF-CHEM and GEM-MACH models show positive values of the mean difference in winter and negative mean differences in the summer, and the WRF-CMAQ summer simulations also show negative mean

differences. The incorporation of feedbacks increases winter temperatures and decreases summer temperatures. Low hourly correlation coefficients across the grid (Figure 1 d,e,f) indicate times when the feedback and no-feedback models have diverged. The correlation coefficient in Figure 1 thus show that the feedbacks have the greatest impact in 2010 from February 15 through March 15, and for a few days centered on April 20th and May 15th. The WRF-CMAQ and GEM-MACH models also show the mid-summer period between July 15th and August 15th as being strongly impacted by feedbacks, though to differing degrees. The WRF-CMAQ differences are much smaller than the other two models; WRF-CMAQ as implemented here includes only the aerosol direct effect, indicating that the indirect effect may have a larger impact on temperature forecasts.

Figure 2 shows the time series of the mean differences (a,b) and correlation coefficients (c,d) for each European (EU) model for the year 2010. The aerosol direct effect decreases the mean surface temperature (Fig. 2(a), red line, always negative), and reaches a maximum perturbation of -0.25C between July 25th and August 19th. This time period also shows as a negative spike in the correlation between feedback and no-feedback simulations for this model (Fig. 2(c)). During the given time period a series of intense forest fires took place in western Russia, the emissions from which were included in the models' emissions database for the EU simulations. In contrast, the indirect + direct effect simulation mean differences (Fig. 2(b)), while also showing a negative value during that time period, are slightly reduced in magnitude relative to the direct effect simulation (note that the scales differ between the figures). The drop in feedback versus no-feedback correlation coefficient so prominent in the direct-effect-only simulation (Fig. 2(c)) appears to be absent when the indirect effect is also included (Fig. 2(d)). However, the overall perturbations in the no-feedback to feedback correlation coefficient when the indirect effect is included are much larger. The impact of the Russian fires with respect to surface temperature is larger for the direct effect, but is modified by indirect effect perturbations when the latter is added. However, there are other meteorological variables for which the indirect effect, driven by the Russian fires, has a dominating influence, as will be shown below.

1.2 Downward flux of shortwave radiation at the surface

The three models' response of downward surface short-wave radiation towards feedbacks differs, as shown in Figure 3. Differences between feedback and non-feedback simulated grid mean values for GEM-MACH (Fig 3(a)) were both positive and negative over the course of the simulation period (with the negative changes having the higher magnitudes). However, for both WRF-CHEM and WRF-CMAQ (Fig. 3(b,c)), the incorporation of feedbacks resulted in reduced downward shortwave fluxes. This difference in response can be explained in the context of the default model options in the absence of feedbacks. In GEM-MACH's non-feedback configuration, aerosol radiative effects are treated through the use of tables of "typical" aerosol radiative properties (AOD, single scattering albedo and backscattering ratio). The mean differences shown for GEM-MACH are differences from these typical conditions, in addition to showing the effects of feedbacks. Positive values in Figure 3(a) thus represent times wherein the feedback aerosols have smaller optical depths than the standard profiles, while negative values indicate times when the feedback aerosols have greater optical depths than the standard profiles. For the WRF-CMAQ and WRF-CHEM simulations, aerosol radiative adjustments are only made in the feedback case (no aerosol radiative effects are assumed in the non-feedback case), hence the impacts on downward shortwave radiation at the ground are all negative. All three models show that feedbacks alter the shortwave radiation travelling towards the ground. The GEM-MACH simulations suggest that while the default optical parameters used in the weather forecast model are within the range of positive and negative variation afforded by explicitly simulated aerosols, there are locally large positive and negative deviations of the radiative balance relative to this case (feedback-induced variations in hourly grid mean values of +10 to -50 Wm^{-2}). The WRF-CHEM and WRF-CMAQ simulations show that the net effect of the aerosols is to decrease the downward radiative flux (by up to -150 and -12 W m^{-2}, respectively).

Correlation coefficients (Fig. 3(d,e,f) show a trend similar to that of temperature (Figure 1), with the summer period from July 15 through August 15th having the greatest impact of feedbacks (i.e. the

lowest correlation between feedback and non-feedback runs). Figure 3(g,h,i) shows the extent to which feedbacks have influenced the hourly spatial variability of the model predictions for temperature, through calculating the difference in the hourly standard deviation of the model results (Feedback standard deviation – Non-Feedback standard deviation). The variability generally increases for GEM-MACH with the incorporation of feedbacks, while increases and decreases during the year can be seen for WRF-CHEM and the variability always decreases for WRF-CMAQ. Given that WRF-CMAQ in this implementation only includes the aerosol direct effect, the increases in variability in surface downward shortwave radiation with the other two models may relate to the changes in the variability of the location of clouds (i.e., the aerosol indirect effect).

The prominent feature of the EU direct-effect-only simulation is the Russian fires, which cause a grid average decrease in the downward flux of -22 Wm^{-2} (Fig. 4 (a)), and a negative spike in the Feedback to No-Feedback model to model correlation coefficient (Fig. 4 (c)). In the simulation incorporating the direct + indirect effects (Fig. 4 (b,d)), the negative perturbation has decreased to -12 Wm^{-2}, and are offset by positive perturbations of greater magnitude (Fig. 4 (b)). These perturbations associated with changes in cloudiness following the incorporation of the aerosol indirect effect dominate the correlation coefficient differences in Figure 4 (d)). The direct effect thus acts to solely reduce the downward shortwave reaching the surface, while the addition of the indirect effect has the potential to increase it, and may offset or reverse the decreases associated with the direct effect. These findings have relevance towards the study of short-term climate forcers – this competition between direct and indirect effect on the radiative balance may have a key role on the impact of aerosols on climate.

1.3 Upward flux of shortwave radiation at the surface

For GEM-MACH, the mean difference in surface upward shortwave radiation varies between +5 and -15W m^{-2}, with no pronounced seasonality, while for the other two NA models, the feedback-induced change in the upward flux is negative, and is higher in the winter than in the summer (WRF-CHEM: up to

-40Wm^{-2}; WRF-CMAQ: up to -2.0 Wm^{-2}; Figure 5, (a) - (c)). The uniform reduction in surface upward shortwave radiation in the latter two models with the addition of feedbacks probably reflects the absence of a parameterization for aerosol radiative transfer in the underlying meteorological model; the upward shortwave flux is reduced in the presence of aerosols, relative to their absence. The positive and negative differences for the GEM-MACH model represent the deviations of the grid average aerosol radiative transfer from the parameterized radiative transfer in the non-feedback simulation. Of potential interest is the extent to which feedbacks modify the variability of simulated meteorological variables such as shortwave radiative fluxes – here, we examine this through the changes in standard deviation of the model fields at each hour (Fig. 3 (g),(h),(i)). Changes in standard deviation of the grid-mean upward flux of shortwave radiation at the surface were mostly positive for GEM-MACH (+5 to -15 Wm^{-2}), negative in winter and positive in summer for WRF-CHEM (-30 to +35 Wm^{-2}), and always negative for WRF-CMAQ (0 to -1.0 Wm^{-2}, with one -3.5 Wm^{-2} outlier in the winter, Figure 5(g)-(i)). The aerosol indirect effect thus seems to increase the variability of the upward shortwave radiative flux while the direct effect decreases it, though the seasonality of this change differs between the two models in which it is incorporated. These models also show the most negative mean differences in the same period, in the month of February, 2010.

Figure 6 compares the EU domain mean upward shortwave radiation. Without feedbacks, the mean surface upward shortwave has the typical variation with seasonal surface changes (i.e. blue time series, Fig. 6 (a,b)). With the introduction of aerosol direct effect changes (Fig. 6 (a), red line), the upward radiation is reduced, while the further introduction of aerosol indirect effects (Fig. 6 (b), red line)) the change in upward radiation may be positive or negative. Linked to the downward radiation (Fig. 4 (b)): the positive changes represent changes (local decreases) in cloudiness, in turn affecting the amount of downward shortwave radiation reaching the surface, hence the amount returning upwards thereafter. The direct effect correlation coefficient (Fig. 6 (c)) once again is dominated by the Russian fire event, and in the direct + indirect simulation (Fig. 6 (d)), the correlation coefficients are controlled by indirect effect

changes resulting in larger differences between the simulations than with the direct effect alone, while not erasing the impact of the fires. Other low correlation events occur in mid-January and mid-February in both simulations.

1.4 Upward flux of shortwave radiation at the top of the model

The height of the top of the models varies, hence only the sign of the feedback effects will be discussed here. The change in the mean upward flux of shortwave radiation due to feedbacks in GEM-MACH and WRF-CMAQ is predominantly positive: feedbacks increase the upward flux of shortwave radiation at the model top (Figure 7 (a-c)). The correlation coefficients for WRF-CMAQ and GEM-MACH are the lowest in the summer, though WRF-CHEM has relatively little seasonal variation (Fig 7(d-f)).

For the EU, the model-top upward shortwave flux (Figure 8) shows that the influence of feedbacks is the reverse of that of the upward flux at the surface (Figure 6). The direct-effect-only simulation (Fig 8 (a)), shows an increase in the upward shortwave flux, and the addition of the indirect effect results in occasional slight increases, but predominantly decreases. Slightly more shortwave energy is released to space with the aerosol direct effect, and more remains in the system when the indirect effect is added. As for all of the EU radiation figures (2, 4, 6, and 8), the largest impact of the feedbacks occurs during the summer months.

1.5 Planetary Boundary Layer Height

The model correlation coefficients between feedback and non-feedback simulated PBL heights were lowest in the summer in both years (Figure 9). The lowest values in correlation coefficient (GEM-MACH: 0.70, WRF-CHEM: 0.20, WRF-CMAQ: 0.96; Figure 9 (a)-(c)) suggest that the aerosol indirect effect contributes the greater portion of the change in PBL height. The models responded differently to feedbacks, with the PBL generally increasing in GEM-MACH, particularly in winter, and generally increasing in WRF-CHEM in the summer and decreasing in winter, while decreasing in the WRF-CMAQ

summer simulation (Figure 9(d)-(f)). The models incorporating the aerosol indirect effect tended to have both positive and negative changes in the standard deviation, while the one incorporating only the direct effect had uniform decreases in standard deviation (Figure 9(g)-(i)). The aerosol direct effect thus appears to reduce the variability in the PBL height.

The aerosol direct effect has a more significant impact than the indirect effect on EU planetary boundary layer height, in contrast to the radiative balance figures discussed above (Figure 10). The change in PBL height for both simulations (red lines, Fig. 10 (a,b)) is predominantly towards decreases in PBL height for both simulations. Direct effect PBL changes (Fig. 10 (a)) are always negative and, while small positive changes occur with the addition of the indirect effect, the latter also has an overall negative offset relative to its no-feedback simulation. Similarly, the differences in correlation coefficient (Fig. 10 (c,d))) are closer in magnitude for the two simulations than the other EU meteorological variables analyzed above. Once again, the Russian fires stand out, as a time of decreased PBL heights and decreased correlation coefficients.

1.6 Precipitation

The magnitude of mean precipitation and the difference in mean precipitation is higher in WRF-CHEM than in GEM-MACH or WRF-CMAQ (Figure 11 (a-c)). The sign of the models' precipitation response to feedbacks differs, with GEM-MACH showing mostly increases in precipitation, WRF-CHEM showing increases and decreases, and WRF-CMAQ showing mostly decreases. The sign and magnitude of the change in precipitation is thus highly model-dependent. The simulations have the lowest correlation coefficients roughly from July 15th through August 15th (Fig. 11 (d-f)), corresponding to the time of greatest photochemical production of aerosols.

The aerosol direct effect only EU simulation generally results in precipitation decreases (Fig. 12(a), red line). Decreases also occur with the addition of the indirect effect, but these are offset by sporadic increases in precipitation which may be a factor of 2 to 3 larger than the decreases associated

with the direct effect (Fig. 12(b)). Both the direct and indirect effects have the biggest impact in the summer, as shown by the seasonality of the correlation coefficients (Fig. 12(c,d)). However, the correlation coefficients are lower on average for the indirect+direct effect simulation (Fig. 12 (d)), despite the Russian fires having a larger impact in the direct effect simulation for a short time period (Fig. 12(c)), again suggesting the indirect effect may dominate.

The WRF-CHEM simulations in the NA domain make use of the Chapman *et al* (2009) implementation of Abdul-Razzak and Ghan (2002)'s aerosol activation scheme, while the GEM-MACH and EU WRF-CHEM indirect+direct effect simulations also make use of Abdul-Razzak and Ghan (2002). The WRF-CHEM/NA model implementation seems to be much more sensitive to feedbacks for its precipitation production than either GEM-MACH or WRF-CHEM/EU, comparing magnitudes of mean differences. Gong et al (2014) found that the Abdul-Razzak and Ghan scheme is very sensitive to the details of the implementation; such implementation differences, as well as the particular cloud microphysics algorithm used, may account for the variation in response seen here.

1.7 Cloud liquid water path

This variable was only available from the GEM-MACH simulation in NA, but is mentioned here due to the large impacts of feedbacks on that parameter. With the inclusion of feedbacks, the cloud liquid water path increased significantly, usually by a factor of two or more (Figure 13 (a)). As with several other meteorological variables, the lowest correlation coefficients occur in the summer (Figure 13(b)), indicating an important seasonality to the feedback effects. In this model, the inclusion of aerosol direct and indirect effects results in an increase in the amount of precipitation and in the amount of cloud liquid water. The cloud droplet number density in the column also increases significantly, in part due to a low droplet number density being assumed in the no-feedback model's original microphysics and the manner in which aerosol bins are subdivided within model parameterizations. These effects are examined in detail in the companion paper by Gong *et al* (2014).

The EU cloud liquid water path changes are compared in Figure 14, and may be contrasted with Figure 13 (liquid water path for North America). The changes in liquid water path for the EU domain associated with the direct effect are very small (Fig. 14(a), compare mean value blue line with red mean difference line). The incorporation of the aerosol indirect effect (Fig. 14(b)) has resulted in a decrease in the liquid water path by a factor of 0.7 to 0.3 depending on time of year. This may be contrasted with the GEM-MACH simulations of Figure 13, where the cloud liquid water path increased significantly. Differences in cloud microphysics modules may account for some of these differences: in the module used in GEM-MACH (Milbrandt and Yao, date) cloud condensation does not occur until the entire grid-box is saturated. In the case of WRF-CHEM as implemented here, the default no-feedback model assumes a constant cloud droplet number in the microphysics scheme. While some of these differences are doubtless due to differences in the methodology used in the respective models, it should also be recalled at this point that the GEM-MACH comparison is between a representative climatological aerosol indirect effect and a fully coupled indirect effect, while the EU WRF-CHEM result (Fig. 14(b,d)) represents the difference relative to an atmosphere with no aerosol direct effects and a prescribed cloud droplet number The GEM-MACH NA simulation thus suggests the cloud water liquid path will increase relative to its parameterized aerosol representation, while the WRF-CHEM EU simulation suggests that in the absence of aerosol indirect effect feedbacks, cloud liquid water path will decrease. However, these findings may be heavily influenced by the parameterization choices within the cloud microphysics schemes used in the no-feedback models and the manner in which aerosols are used to modify those schemes in the feedback simulations. At the same time, the differences between the model responses likely also represents difference in the implementation of indirect effects, in that the climatological "no-feedback" simulation of GEW-MACH (blue line, Fig. 13(a)) has typical average values on the order of 120 m, with feedbacks increasing that by 100m or more, while the WRF-CHEM EU feedback simulations have typical levels of about 70m, once the feedbacks have been taken into account. Sensitivity simulations with the GEM-MACH model (Gong *et al*., 2014, this volume) show that the cloud properties of fully coupled models are highly sensitive to the assumptions regarding updraft statistics and aerosol

size distribution in determining cloud condensation nuclei numbers. Comparisons between the available parameterizations and highly time and space resolved cloud studies are needed to evaluate and improve these parameterizations.

2. Spatial Analysis of Feedbacks

In this section, we analyze the model results over time at each model gridpoint, rather than over space. The model-to-model comparison statistics are described in Table 2, where N is now the number of hours of comparison times at each gridpoint, rather than the number of common AQMEII-2 NA or EU gridpoints used in the time series comparison. To illustrate the differences, example meteorological fields' mean differences and correlation coefficients will be shown to identify the regions with the greatest impact of feedbacks. This portion of the analysis pairs NA and EU contour maps of feedback influences. The maps were generated for the period July 15th through August 15th , 2010 for the NA domain, and July 25th through August 19^{th,} 2010 for the EU domain, in order to allow all three models to be compared for NA, and to focus on the Russian fires period for EU.

2.1 Downward Shortwave Radiation and Temperature

For the meteorological variables, all five models can be compared. Figure 15 shows the change in mean downward shortwave radiation and mean surface temperatures for the NA models, with the EU model differences shown in Figure 16.

GEM-MACH (Figure 15(a)), where the no-feedback simulation includes climatological parameterizations for aerosol radiative and cloud condensation nucleation, has both increases and decreases, with the maximum increase between +15 to +25 Wm^{-2} along the California/Nevada border, while decreases of up to -45 Wm^{-2} take place over the Pacific ocean, Hudson's Bay, the Atlantic ocean, over large parts of the provinces of Ontario and Quebec, and at isolated locations in the USA. These locations likely represent regions where the aerosol distribution generated by the model is significantly different from the parameterized aerosols used in the no-feedback GEM-MACH simulation. WRF-CHEM (Fig. 15 (b),

direct+indirect effect, no climatological parameterizations), like WRF-CMAQ, also had slight increases in the center of the continent, but much larger decreases on the western boundary and eastern half of the domain. WRF-CMAQ (Fig. 15(c), direct effect, no climatological parameterizations), gave a smaller dynamic range of radiation differences, predominantly negative, over the western and eastern portions of the continent, with the largest decreases on the order of -12 W m^{-2}.

Temperature changes over NA show a similar pattern; all models tend towards decreases in temperature, though the spatial distribution changes; for GEM-MACH (Fig. 15 (b)) the decreases occur over the eastern half of the shared domain and along the west coast, for WRF-CMAQ (Fig. 15 (f)) the decreases are patchy over the center of the continent, with increases to the north-west and north-east, and for WRF-CHEM (Fig. 15 (d)) large decreases occur over the western part of the domain, and smaller decreases over most of the continent, with small increases over Alberta, Montana, Ontario and Quebec.

These meteorological changes (decreases in shortwave radiation and temperature over much of NA) help explain biogenic isoprene concentration differences noted in Makar *et al*., (2014) (Part 2): both radiative and temperature drivers of isoprene emissions have decreased with the incorporation of feedbacks, resulting in decreases in isoprene concentrations.

The EU simulations of downward shortwave radiation and surface temperature in Figure 16 both show the impact of the Russian fires, but this impact is stronger in the direct effect model (Fig. 16 (a,b)) than in the direct+indirect effect model (Fig. 16 (c,d) – compare scales between (a,c) and (b,d)). For the direct effect simulation, the fires result in reductions of up to -80 Wm^{-2} and -0.8 ^{o}C. In contrast, the direct+indirect effect simulation (Fig. 16 (c,d)) shows a relatively minor changes, with decreases of a few W m^{-2} and maximum temperature decreases of -0.1 ^{o}C. Both simulations show decreases in downward shortwave radiation over much of Europe – the indirect+direct effect simulation suggests that these will be accompanied by temperature increases of up to 0.1 C, while the direct effect causes temperature decreases. The implication is that the indirect effect is once again dominating, capable of reversing

changes caused by the direct effect, as well as having a substantial impact on the model's response to forest fires.

2.2 Planetary Boundary Layer Height

The change in PBL height during the summer period for the models is shown in Figure 17. In NA (Fig. 17 (a-c), the response of models to the feedbacks varies greatly (the same colour scale is used for all NA models). The PBL height generally increases in the GEM-MACH simulation relative to the run with climatological aerosol effects (Fig. 17 (a)), while the direct effect WRF-CMAQ simulation's PBL height slightly decreases (Fig. 17 (b)), and the WRF-CHEM PBL height decreases over most of the domain, aside from the north-east and north-west parts of the domain, where large increases occurred. The GEM-MACH changes reflect the local impacts of the model-generated aerosols: PBL increases significantly (+10 to +30%) over the northern Great Lakes, Hudson's Bay, and the California coast. The WRF-CHEM/NA simulation's PBL has a sharp delineation between positive and negative changes. In Europe, the direct effect only simulation (Fig. 17(d)) shows large decreases (> -30%) in the centre of the Russian fire region, and relatively smaller changes elsewhere. The indirect effect model (Fig. 17 (e)) also shows decreases of (> -30%) for the Russian fires, as well as some regions of PBL height increase (coast of Iceland, >+30%). All of the models are thus showing an impact of feedbacks on PBL height, ranging from +/-3% for the direct effect WRF-CMAQ to +/-30% for the other models. The emissions from the Russian fires in the EU simulations have resulted in a significant drop in both direct effect and indirect effect simulations, implying that the effect there may be dominated by the direct effect, or that the net impact of the direct and indirect+direct effects is similar. In contrast, in NA the model employing only the direct effect (Fig. 17 (b)) has a much lower response of PBL height to feedbacks (compare to Fig.17 (a,c)).

2.3 Precipitation

Changes in mean precipitation during the summer periods due to feedbacks are shown in Figure 18. The net changes in precipitation across the grid (Figures 11, 12) are very spatially heterogeneous, aside from a few hot-spots. In NA (Fig. 18 (a-c), the models combining direct and indirect effects (a,c) have a greater range in precipitation differences than the direct effect model. For the EU models, the dynamic range of local precipitation changes is only slightly larger for the direct+indirect simulation (e) compared to the direct effect simulation (d). In Europe, the Russian fires have resulted in a net decrease in precipitation.

2.4 Cloud Liquid Water Path

Changes in the mean cloud liquid water path were available for three models, GEM-MACH, and the two EU WRF-CHEM simulations, shown in Figure 19. The direct effect EU simulation (Fig. 19 (b)) shows the smallest changes, likely associated with shifts in cloud position. The two direct + indirect feedback simulations have a much larger response. For the GEM-MACH simulation (Fig. 19 (a)) cloud liquid water path predominantly increases. For the WRF-CHEM simulation (Fig. 19 (c)), cloud liquid water path decreases. Both models made use of the Abdul-Razzak and Ghan (2002) scheme for estimating aerosol activation, however both this scheme and the cloud microphysics parameterizations which employ it are sensitive to the details of implementation; these will be updated and improved in future versions of GEM-MACH (Gong *et al*, 2014, this issue). GEM-MACH's differences reflect changes relative to that model's parameterized climatology approach to cloud condensation nucleation – positive values representing increases relative to the parameterization, negative values representing decreases. However, the difference in the dynamic range (maximum-minimum) of the changes between the models (580 gm^{-3} for GEM-MACH, 300 gm^{-3} for WRF-CHEM) suggest important differences in implementation, which should be investigated in future work.

3. Summary of Feedback Effects

The main results of the time series and spatial comparisons are summarized in Table 3 and 4.

Table 3 shows the lowest hourly spatial correlation coefficient between feedback and no-feedback simulations for the models studied here, in North America and Europe respectively. It is apparent from these values that the feedbacks can at times have a very significant impact on the hourly spatial distribution of meteorological variables, resulting in relatively low spatial correlations between feedback and no-feedback simulations. The correlations are lowest for the precipitation-related variables, reflecting changes in the spatial pattern of clouds being created by the feedback and no-feedback simulations. Temporal averages plotted across the continent (Figures 15 through 21) show that the impact of the feedbacks vary spatially, and are often associated with large sources of emissions.

Table 4 gives the broadest possible summary of the impacts for the different meteorological variables compared; whether the feedback effects increased or decreased that variable, and seasonality effects, when the latter are pronounced. Some common effects may be seen across models and domains. Those models which implement only the direct effect feedback had resulting decreases in temperature, surface downward and upward shortwave radiation, precipitation, and PBL height, and increases in upward shortwave radiation. The feedback response of the models incorporating both direct and indirect effects ("D+I" in Table 4) varied with the model and simulation domain, indicating a more complex response and, possibly, a greater dependence on the manner in which the indirect effect is implemented. For example, North American temperatures increased in the winter and decreased in the summer with the combined direct and indirect effect models, while the European temperatures had the reverse trend. North American WRF-CHEM surface downward shortwave radiation decreased, while no trend was noticeable for the other D+I models. All D+I models showed no clear trend in in surface upward shortwave radiation. The North American D+I model feedbacks increased upward shortwave at the model top; while this decreased for the European D+I model. North American D+I precipitation mainly increased relative to the no-feedback simulation, while in Europe there was less of a trend towards increases. PBL height decreased in Europe for the D+I simulation, while decreasing in summer and increasing in winter for the North American simulations. The models thus show similar impacts for the direct effect, but for

526 the combined direct + indirect effect, the response is much more variable. A consequent recommendation
527 of this work is that the details of implementation of the indirect effect across models should be re-
528 examined, for specific short-term case studies.

529

530 4. Impacts relative to observations.

531 A detailed analysis of the model generated meteorology for the year 2010 for the NA and EU grids is
532 presented in Brunner et al, (2014), for those simulations which were carried out over an entire year. No-
533 feedback annual simulations for North America were not carried out for WRF-CHEM and WRF-CMAQ,
534 though their feedback simulations were evaluated. Some of the key results of that analysis with regards to
535 the portion of the AQMEII-2 models participating in this feedback and no-feedback comparison will be
536 briefly mentioned here (see mean bias Tables 5 and 6, and Figures 20 and 21, and cf. Brunner et al.
537 (2014) for an overview of performance for all participating AQMEII-2 models). The magnitudes of the
538 biases within a given model can be seen by comparing the two GEM-MACH columns in North America
539 in Table 5, and by comparing the two WRF-CHEM5.4.1 columns of Table 6. These may be contrasted
540 with the magnitude of the mean biases reported in the remaining columns of these tables, for the other
541 models. The differences associated with implementing feedbacks *within* a given model are usually smaller
542 than the differences in mean bias *between* different models or model versions. This finding is consistent
543 with those of the chemical analysis portion of this two-part paper (Makar et al, 2014), and indicates that
544 the impacts of other model parameterizations may have a larger influence on overall model performance
545 than feedbacks. However, within a given model for which both feedback and non-feedback simulations
546 were available, the use of feedbacks sometimes resulted in significant changes to performance, as is
547 evidenced by the first two columns of Tables 5 and 6. The use of feedbacks in the GEM-MACH model
548 (Table 5, first two columns) reduced the bias of the annual surface pressure, 2 m temperature, and
549 precipitation, while resulting in a slight increase in the bias of annual wind . The improvements in
550 precipitation bias are of note (biases reduced by 13%, 20% and 30% going from western to north-eastern

North America) given that GEM-MACH's negative precipitation bias was larger than that of the other models compared here. It should be noted that the overall negative biases in GEM-MACH precipitation stem in part from the use of an explicit 2 moment cloud microphysics scheme for a model spatial resolution of 15km, in the implementation used here. The spatial pattern of the changes in the mean annual temperature bias relative to observation in North American (GEM-MACH, direct + indirect effect) and Europe (WRF-CHEM, direct effect) are shown in Figures 20 and 21, respectively. The magnitude of the bias has decreased over most of North America (Figure 20), with the greatest improvements over western NA, and some increases in bias in the north-central portion of the domain. Improvements in 2m temperature biases associated with the inclusion of the direct effect in WRF-CHEM for Europe are shown in Figure 21; these extend over most of the domain, and are greatest in the industrial and population centers of Great Britain, France, Germany, Belgium, The Netherlands, Spain and Austria.

For the EU domain (Table 6) there were significant improvements in annual 2m temperature, going from the WRF-CHEM 5.4.1 no-feedback simulation to the corresponding WRF-CHEM5.4.1 direct-effect only simulation. The direct effect had no discernable impact on annual wind speed. The WRF-CHEM 5.4.0 simulation (which included both direct and indirect effects) had the best overall performance for temperature, but relatively poor performance for wind speed.

These comparisons (see Brunner et al, 2014, for a complete evaluation of all AQMEII-2 models) suggest that feedbacks have the potential to improve weather forecasts, though the large model-to-model differences suggest that other details of model implementation may have an effect as significant or larger than the feedbacks, depending on the meteorological variable being considered. The feedback effect for short-term weather forecasts is therefore subtle, but capable of improving model forecasts.

Summary and Conclusions

In our Introduction, we posed three questions regarding the effects of feedbacks on forecasts of chemistry and meteorology. The impacts on chemistry are discussed in Part 2 (Makar et al, 2014). We return to the questions here in the context of meteorological forecasts.

(1) *The incorporation of feedbacks results in systematic changes to forecast predictions of meteorological variables*. Hourly spatial correlation coefficients between feedback and no-feedback simulations for several meteorological variables tend to show the largest near-surface impacts in the summer. This corresponds to the time of greatest photochemical activity and secondary particle formation.

(2) *The changes associated with feedbacks vary in both time and space* – temporally, the changes are the most closely associated with summer photochemical production, and with time of high emissions (such as large forest fires). Spatially, the regions with the greatest impact of feedbacks tend to be associated with large emission sources such as the Russian fires, though significant spatial changes could be observed elsewhere. Decreases in downward shortwave radiation at the surface in comparison to no-feedback models lacking climatological aerosols in North America show the largest decreases in the eastern USA and Canada, corresponding to the regions of highest anthropogenic particle loading. Both direct and indirect+direct effect North American simulations relative to a "no aerosol climatology parameterization" no-feedback state resulted in decreases of downward shortwave radiation at the surface over most of the domain – the simulation relative to parameterized aerosol properties showed increases in surface downward shortwave radiation in the western and Midwestern USA. Summer 2010 European temperatures and all other meteorological variables were strongly influenced by the Russian forest fires: EU direct-effect only simulations had the largest shortwave decrease (maximum -80 W m^{-2}, compared to -10 W m^{-2} for direct+indirect effects). The EU indirect effect simulation showed temperature increases (maximum +0.2 ^{o}C) over much of Europe, with the largest increases along

coastal Iceland, Norway, northern Great Britain and Ireland, the mountainous regions of central and south-west Europe, and the north-west coast of Africa. Feedbacks were thus shown to result in both temporal and spatial variations in model forecasts.

(3) *The extent to which the models improve or worsen weather forecast results is variable, at the current stage of feedback model development*. The difference in mean bias resulting from the incorporation of feedbacks within a given model was found to be smaller than the differences in mean bias between different models. However, within a given model, the feedback effects were sufficiently strong to result in improvements to some meteorological variable biases relative to observations (improvements in forecasted temperature and precipitation in North America for direct + indirect effect simulations, and temperature for direct effect simulations within Europe). The feedback effects may therefore be said to be subtle, given the differences across models, yet capable of improving model forecasts, even at this early stage in coupled air-pollution / weather forecast model development. Further work is clearly needed to improve both the driving model meteorological parameterizations and the manner in which feedbacks are simulated within the models.

Models incorporating just the direct effect showed feedback-induced reductions in temperature, surface downward and upward shortwave radiation, precipitation, and PBL height, and increases in upward shortwave radiation. Models making use of both direct and indirect feedbacks had larger variations in response to feedbacks; for example, both combined effect models in North America showed increases in summer temperatures and decreases in winter temperatures, while the combined effect model for Europe showed the opposite seasonal trend. Some of the variation in model response for the indirect effect may reside in differences in the no-feedback base case (one model, GEM-MACH, employed simple parameterizations for aerosol radiative properties and cloud condensation nuclei formation in its no-feedback mode, while the others had a “no aerosol” atmosphere, for the no-feedback simulation). However, the variation in response suggests that further work comparing the methodologies and

623 parameterizations used to represent the indirect effect should take place, given the variety of response
624 seen here.

625 The variation in model response to feedbacks in the combined direct and indirect effect models was the
626 most pronounced for cloud and precipitation variables. For example, the GEM-MACH and WRF-
627 CHEM/EU models showed substantial feedback-induced increases in precipitation in both continents,
628 while the WRF-CHEM/NA model showed decreases in precipitation. The European simulation cloud
629 liquid water paths decreasing significantly and the North American cloud liquid water paths increased or
630 decreased depending on location. All three models employed the Abdul-Razzak and Ghan (2002) scheme
631 for cloud condensation nucleation, though the microphysics modules employing the scheme differ in
632 construction and underlying assumptions. The precipitation and cloud property responses to feedbacks
633 were thus shown to be dependent on the details of implementation of both aerosol activation and cloud
634 microphysics. These sensitivities are examined elsewhere in this issue (Gong et al, 2014). A process-
635 oriented cross-comparison of indirect effect implementations, including the microphysics schemes
636 employed and the extent of aerosol interactions with those schemes, for shorter-duration test cases, is
637 therefore recommended for future research.

638 Our results suggest that the aerosol indirect effect usually dominates over the aerosol direct effect, given
639 that models incorporating both show feedback-derived changes which are substantially larger than those
640 of with the direct effect alone (cf. our time series for surface 2m temperature, downward and upward
641 shortwave radiation at the surface, upward shortwave radiation at the model top, PBL height in North
642 America, precipitation and cloud liquid water path all show a greater magnitude decreases in correlation
643 coefficient for models incorporating the indirect effect than direct-effect only models). The
644 comparisons also suggest that the direct and indirect effects may sometimes act in *competition* (c.f. our
645 EU time series for 2m temperature, surface downward and upward shortwave radiation, model top
646 upward shortwave radiation, and PBL height, and compare the direction of changes for the same variables

between NA direct + indirect effect models with the direct effect model). Studies focused on the processes by which that competition takes place are recommended for future research.

Acknowledgements

The authors gratefully acknowledge funding from Environment Canada's Clean Air Regulatory Agenda. The Centre of Excellence for Space Sciences and Technologies SPACE-SI is an operation partly financed by the European Union, European Regional Development Fund and Republic of Slovenia, Ministry of Higher Education, Science, Sport and Culture. G. Curci and P. Tuccella were supported by the Italian Space Agency (ASI) in the frame of the PRIMES project (contract n. I/017/11/0)."

References

Abdul-Razzak, H. and Ghan,S.J., 2002. A parameterization of aerosol activation 3. Sectional representation. *Journal of Geophysical Research, Atmospheres*, 107, D3, pp AAC-1-1 to AAC1-6, DOI 10.1029/2001JD000483.

Ackerman, I. J., H. Hass, M. Memmesheimer, A. Ebel, F. S. Binkowski, U. Shankar,1998. Modal aerosol dynamics model for Europe: development and first applications, Atmospheric Environment, 32, 17, 2981 – 2999.

Ahmadov, R., S. A. McKeen, A. Robinson, R. Bahreini, A. Middlebrook, J. de Gouw, J. Meagher, E. Hsie, E. Edgerton, S. Shaw, M. Trainer, 2012. A volatility basis set model for summertime secondary organic aerosols over the eastern United States in 2006, J. Geophys. Res., 117, D06301, doi:10.1029/2011JD016831.

Appel, K. W., Pouliot, G. A., Simon, H., Sarwar, G., Pye, H. O. T., Napelenok, S. L., Akhtar, F., and Roselle, S. J., 2013. Evaluation of dust and trace metal estimates from the Community Multiscale Air Quality (CMAQ) model version 5.0, Geosci. Model Dev., 6, 883-899, doi:10.5194/gmd-6-883-2013.

Baklanov, A., Schlunzen, K., Suppan., P., Baldasano, J., Brunner, D., Aksoyoglu, S., Carmichael, G., Douros, J., Flemming, J., Forkel, R., Galmarini, S., Gauss, M., Grell, G., Hirtl, M., Joffre, S., Jorba, O., Kaas, E., Kaasik, M., Kallos, G., Kong., X., Korsholm., U., Kurganskiy, A., Kushta, J., Lohmann, U., Mahura, A., Manders-Groot, A., Murizi, A., Moussiopoulos, N., Rao, S.T., Savage, N., Seigneur, C., Sokhi, R.S., Solazzo, E., Solomos, S., Sorenson, B., Tsegas, G., Vignati, E., Vogel, B., and Zhang, Y., 2014. Online coupled regional meteorology chemistry models in Europe: current status and prospects. Atm. Chem. Phys. 14, 317-398.

677 Bélair, S., L.-P. Crevier, J. Mailhot, B. Bilodeau, and Y. Delage, 2003a. Operational implementation of
678 the ISBA land surface scheme in the Canadian regional weather forecast model. Part I: Warm
679 season results. J. Hydrometeor., 4, 352-370.

680 Bélair, S., R. Brown, J. Mailhot, B. Bilodeau, and L-P. Crevier, 2003b. Operational implementation of the
681 ISBA land surface scheme in the Canadian regional weather forecast model. Part II: Cold season
682 results. J. Hydrometeor., 4, 371-386.

683 Bohren, C.F., and Huffman, D.R., 1983. *Absorption and scattering of light by small particles*, Wiley and
684 Sons, New York, 530 pp.

685 Bohren, Craig F. and Donald R. Huffman, 1998. *Absorption and scattering of light by small particles*,
686 New York: Wiley, 530 p., ISBN 0-471-29340-7, ISBN 978-0-471-29340-8 (second edition)

687 Brunner, D., Savage, N., Jorba, O., Eder, B., Giordano, L., Badia, A., Balzarini, A., Baro, Rocio,
688 Bianconi, R., Chemel, C., Forkel, R., Jimenez-Guerrero, P., Hirtl, M., Hodzic, A., Honzak, L.,
689 Im., U., Knote, C., Kuensen, J.J.P., Makar, P.A., Manders-Groot, A., Neal, L., Perez, J.L.,
690 Pirovano, G., San Jose, R., Schroder, W., Sokhi, R.S., Syrakov, D., Torian, A., Werhahn, J.,
691 Wolke, R.., van Meijgaard, E., Yahya, K., Zabkar, R., Zhang, Y., Hogrefe, C., and Galmarini, S.,
692 Evaluation of the meteoroloogical performance of coupled chemistry-meteorology models in
693 phase 2 of the Air Quality Model Evaluation International Initiative, Atmos. Env., *submitted*.

694 Byun, D. W. and Schere, K. L., 2006. Review of the governing equations, computational algorithms, and
695 other components of the Models- 3 Community Multiscale Air Quality (CMAQ) Modeling
696 System, Appl. Mech. Rev., 59, 51–77.

697 Campbell, P., K. Yahya, K. Wang, Y. Zhang, C. Hogrefe, G. Pouliot, C. Knote, R. San Jose and J. L.
698 Perez, P. J. Guerrero, R. Baro, and P. Makar, 2014, Indicators of the Sensitivity of O_3 and $PM_{2.5}$
699 Formation to Precursor Gases over the Continental United States: A Multi-Model Assessment for
700 the 2006 and 2010 Simulations under the Air Quality Model Evaluation International Initiative
701 (AQMEII) Phase 2, *Atmospheric Environment*, submitted.

702 Chapman EG, WI Gustafson Jr, JC Barnard, SJ Ghan, MS Pekour, and JD Fast, 2009. Coupling aerosol-
703 cloud-radiative processes in the WRF-Chem model: Investigating the radiative impact of large
704 point sources. *Atmos. Chem. Phys.*, 9:945-964.

705 Chen, F. and J. Dudhia, 2001. Coupling an advanced land-surface/hydrology model with the Penn
706 State/NCAR MM5 modeling system. Part I: Model implementation and sensitivity. Mon. Wea.
707 Rev., 129, 569-585.

708 Clough, S. A., Shephard, M. W., Mlawer, E. J., Delamere, J. S., Iacono, M. J.,Cady-Pereira, K.,
709 Boukabara, S., Brown, P. D., 2005. Atmospheric radiative transfer modeling: a summary of the
710 AER codes. J. Quant. Spectrosc. Radiat. Transfer 91 (2): 233–
711 244, doi:10.1016/j.jqsrt.2004.05.058.

712 Cohard, J.-M. Pinty, J.-P., and Bedos, C, 1998. Extending Twomey's analytical estimate of nucleated
713 cloud droplet concentrations from CCN spectra. J. Atmos. Sci., 55, 3348–3357.

Ek, M. B., K. E. Mitchell, Y. Lin, E. Rogers, P. Grunmann, V. Koren, G. Gayno, and J. D. Tarpley, 2003. Implementation of Noah land surface model advances in the National Centers for Environmental Prediction operational mesoscale Eta model, J. Geophys. Res., 108, 8851, doi:10.1029/2002JD003296, D22.

Fast, J. D., Gustafson, Jr., W. I., Easter, R. C., Zaveri, R. A., Barnard, J. C., Chapman, E. G., Grell, G. A., and Peckham, S. E., 2006. Evolution of Ozone, Particulates and Aerosol Direct Radiative Forcing in the Vicinity of Houston Using a Fully Coupled Meteorology-Chemistry-Aerosol Model, J. Geophys. Res., 111, D21305, doi:10.1029/2005JD006721.

Fillion, L., M. Tanguay, E. Lapalme, B. Denis, M. Desgagne, V. Lee, N. Ek, Z. Liu, M. Lajoie, J-F. Coron, C. Pagé, 2010. The Canadian regional data assimilation and forecasting system, Weather and Forecasting, 25, 1645-1669.

Foley, K. M., Roselle, S. J., Appel, K. W., Bhave, P. V., Pleim, J. E., Otte, T. L., Mathur, R., Sarwar, G., Young, J. O., Gilliam, R. C., Nolte, C. G., Kelly, J. T., Gilliland, A. B., and Bash, J. O.,2010. Incremental testing of the Community Multiscale Air Quality (CMAQ) modeling system version 4.7, Geosci. Model Dev., 3, 205–226, doi:10.5194/gmd-3-205-2010.

Forkel, R., Werhahn, J., Hansen, A.B., McKeen, S., Peckham, S., Grell, G., Suppan, P., 2012. Effect of aerosol-radiation feedback on regional air quality – A case study with WRF/Chem. Atmos. Environ., 53, 202-211.

Galmarini, S., Rao, S.T., and Steyn, D.G., 2012a. Preface, Atmospheric Environment Special Issue on the Air Quality Model Evaluation International Initiative, Atmos. Environ., 53, 1-3.

Galmarini, S., Bianconi, R., Appel, W., Solazzo, E., Mosca, S., Grossi, P., Moran, M., Schere, K., Rao, S.T., 2012b. ENSEMBLE and AMET: Two systems and approaches to a harmonized, simplified and efficient facility for air quality models development and evaluation, Atmospheric Environment 53, 51-59.Gong, S. L., Barrie, L. A., and Lazare, M., 2003(a). Canadian Aerosol Module (CAM): A size-segregated simulation of atmospheric aerosol processes for climate and air quality models 2. Global sea-salt aerosol and its budgets, *J. Geophys. Res*., 107, 4779, doi:10.1029/2001JD002004.

Gong, S. L., Barrie, L. A., Blanchet, J.-P., von Salzen, K., Lohmann, U., Lesins, G., Spacek, L., Zhang, L. M., Girard, E., Lin, H., Leaitch, R., Leighton, H., Chylek, P., and Huang, P., 2003(b). Canadian Aerosol Module: A size-segregated simulation of atmospheric aerosol processes for climate and air quality models. 1. Module development, *J. Geophys. Res*., 108, 4007, doi:10.1029/2001JD002002.

Gong, W., Dastoor, A. P., Bouchet, V. S., Gong, S. L., Makar, P. A., Moran, M. D., Pabla, B., Menard, S., Crevier, L.-P., Cousineau, S., and Venkatesh, S., 2006. Cloud processing of gases and aerosols in a regional air quality model (AURAMS), *Atmos. Res*., 82, 248– 275.

Grell, G. A., and D. Dévényi, 2002. A generalized approach to parameterizing convection combining ensemble and data assimilation techniques, Geophys. Res. Lett., 29(14), doi:10.1029/2002GL015311.

Grell, G.A., Peckham, S.E., Schmitz, R., McKeen, S.A., Frost, G., Skamarock, W.C., Eder, B., 2005. Fully coupled online chemistry within the WRF model. Atmos. Environ. 39, 6957-6975.

Grell, G. A. and Freitas, S. R., 2013. A scale and aerosol aware stochastic convective parameterization for weather and air quality modeling, Atmos. Chem. Phys. Discuss., 13, 23845-23893, doi:10.5194/acpd-13-23845-2013..

Hogrefe. C., G. Pouliot, D. Wong, A. Torian, S. Roselle, J. Pleim, and R. Mathur, 2014, Annual Application and Evaluation of the Online Coupled WRF-CMAQ System over North America under AQMEII Phase 2, Atmospheric Environment, under review.

Hong, S.-Y., Y. Noh, and J. Dudhia, 2006. A new vertical diffusion package with an explicit treatment of entrainment processes, Mon. Wea. Rev., 134, 2318-2341.

Iacono, M.J., Delamere, J.S., Mlawer, E.J., Shephard, M.W., Clough, S.A., and Collins, W.D., Radiative forcing by long-lived greenhouse gases: Calculations with the AER radiative transfer models. J. Geophys. Res., DOI: 10.1029/2008JG009944.

Im U., Bianconi, R., Solasso, E., Kioutsioukis, I., Badia, A., Balzasrini, A., Brunner, D., Chemel, C., Curci, G., Davis, L., van der Gon, H.D., Esteban., R.B., Flemming, J. Forkel, R., Giordano, L., Geurro, P.J., Hirtl, M., Hodsic, A., Honzka, L., Jorba, O., Knote, C., Kuenen, J.J.P, Makar, P.A., Manders-Groot, A., Pravano, G., Pouliot, G., San Jose, R., Savage, N., Schorder, W., Syrakov, D., Torian, A., Werhan, J., Wolke, R., Yahya, K., Žabkar, R., Zhang, J., Zhang, Y., Hogrefe, C., Galmarini, S., 2014a. Evaluation of operational online-coupled regional air quality models over Europe and North America in the context of AQMEII phase 2. Part I: Ozone, Atmos. Environ. *submitted.*

Im U., Bianconi, R., Solasso, E., Kioutsioukis, I., Badia, A., Balzasrini, A., Brunner, D., Chemel, C., Curci, G., Davis, L., van der Gon, H.D., Esteban., R.B., Flemming, J. Forkel, R., Giordano, L., Geurro, P.J., Hirtl, M., Hodsic, A., Honzka, L., Jorba, O., Knote, C., Kuenen, J.J.P, Makar, P.A., Manders-Groot, A., Pravano, G., Pouliot, G., San Jose, R., Savage, N., Schorder, W., Syrakov, D., Torian, A., Werhan, J., Wolke, R., Yahya, K., Žabkar, R., Zhang, J., Zhang, Y., Hogrefe, C., Galmarini, S., 2014a. Evaluation of operational online-coupled regional air quality models over Europe and North America in the context of AQMEII phase 2. Part 2: Particulate Matter, Atmos. Environ. *Submitted*

IPCC (2007): Intergovernmental Panel on Climate Change (IPCC): Special Report on Emissions Scenarios, edited by: Nacenovic, N. and Swart, R., Cambridge Univ. Press, New York, 612 pp., 2000. Intergovernmental Panel on Climate Change (IPCC): Summary for Policymakers, in: Climate Change 2007: The Physical Science Basis. Contribution of Working Group I to the Fourth Assessment Report of the Intergovernmental Panel on Climate Change, edited by: Solomon, S., Qin, D., Manning, M., Chen, Z., Marquis, M., Averyt, K. B., Tignor, M., and Miller, H. L., Cambridge University Press, Cambridge, 12–17.

Kain, J.S. and Fritsch, J.M., 1990. A one-dimensional entraining/detraining plume model and its application in convective parameterizations, *J. Atmos. Sci*.,47, 2784-2802.

Kain, J. S.: The Kain-Fritsch convective parameterization: an update, 2004. *J. Appl. Meteorol.*, 43, 170–181.

Li, J. and H. W. Barker, 2005. A radiation algorithm with correlated k-distribution. Part I: local thermal equilibrium. *J. Atmos. Sci*, 62, 286-309.

Lurmann, F. W., Lloyd, A. C. Atkinson, R., 1986. A chemical mechanism for use in long-range transport/acid deposition computer modeling. Journal of Geophysical Research 91, 10,905-10,936.

Mailhot, J. and R. Benoit, 1982. A finite-element model of the atmospheric boundary layer suitable for use with numerical weather prediction models. *J. Atmos. Sci*, 39, 2249-2266.

Mailhot, J., S. Bélair, L. Lefaivre, B. Bilodeau, M. Desgagné, C. Girard, A. Glazer, A-M. Leduc, A. Méthot, A. Patoine, A. Plante, A. Rahill, T. Robinson, D. Talbot, A. Tremblay, P. Vaillancourt, A. Zadra and A. Qaddouri, 2006. The 15-km version of the Canadian regional forecast system, *Atmosphere-Ocean*, 44, 133-149.

Makar, P.A., Gong, W., Hogrefe, C., Zhang, Y., Curci, G., Zakbar,Milbrandt, J., , Im, U., Galmarini, S., Balzarini, A., Baro, R., Bianconi, R., Cheung, P., Forkel, R., Gravel, S., Hirtl, M., Honzak, L., Hou, A., Jimenez-Guerrero, P., Langer, M., Moran, M.D., Pabla, B., Perez, J.L., Pirovano, G., San Jose, R., Tuccella, P., Werhahn, J., Zhang, 2014. Feedbacks between Air Pollution and Weather, Part 2: Effects on Chemistry. *Under Review, Atmos. Environ*.

Milbrandt, J.A. and M.K. Yau, 2005(a). A multimoment bulk microphysics parameterization. Part I: analysis of the role of the spectral shape parameter. *J. Atmos. Sci*., 62, 3051-3064.

Milbrandt, J.A. and M.K. Yau, 2005(b). A multimoment bulk microphysics parameterization. Part II: A proposed three-moment closure and scheme. *J. Atmos. Sci*., 62, 3065-3081.

Moran M.D., S. Ménard, D. Talbot, P. Huang, P.A. Makar, W. Gong, H. Landry, S. Gravel, S. Gong, L-P. Crevier, A. Kallaur, M. Sassi, 2010. Particulate-matter forecasting with GEM-MACH15, a new Canadian air-quality forecast model. In: Steyn DG, Rao ST (eds) *Air Pollution Modelling and Its Application XX*, Springer, Dordrecht, pp. 289-292.

Morrison, H., G. Thompson, V. Tatarskii, 2009. Impact of Cloud Microphysics on the Development of Trailing Stratiform Precipitation in a Simulated Squall Line: Comparison of One- and Two-Moment Schemes. *Mon. Wea. Rev.*, 137, 991–1007.
doi: http://dx.doi.org/10.1175/2008MWR2556.1

Pleim, J. E., 2007a. A combined local and nonlocal closure model for the atmospheric boundary layer. Part I: model description and testing, J. Appl. Meteorol. Clim., 46, 1383–1395.

Pleim, J. E., 2007b. A combined local and nonlocal closure model for the atmospheric boundary layer. Part II: application and evaluation in a mesoscale meteorological model, J. Appl. Meteorol. Clim., 46, 1396–1409.

Sarwar, G., Appel, K. W., Carlton, A. G., Mathur, R., Schere, K., Zhang, R., Majeed, M. A., 2011. Impact of a new condensed toluene mechanism on air quality model predictions in the US. Geoscientific Model Development, 4, 183-193.

Sauter, F., van der Swaluw, E., Manders-Groot, A., Wichink Kruit, R, Segers, A., Eskes, H., 2012. LOTOS-EUROS v1.8 Reference Guide. TNO report TNO-060-UT-2012-01451, TNO.

Schell B., I.J. Ackermann, H. Hass, F.S. Binkowski, and A. Ebel, 2001. Modeling the formation of secondary organic aerosol within a comprehensive air quality model system, Journal of Geophysical research, 106, 28275-28293.

Skamarock, W. C., Klemp, J. B., Dudhia, J., Gill, D. O., Barker, D. M., Duda, M. G., Huang, X.-Y., Wang, W., and Powers, J. G., 2008. A description of the Advanced Research WRF version 3, National Center for Atmospheric Research Tech. Note, NCAR/TN- 475+STR, 113 pp.

Stockwell, W. R., Kirchner, F., Kuhn, M., Seefeld, S., 1997. A new mechanism for regional atmospheric chemistry modeling. Journal of Geophysical Research, 102, 25847-25879.

Wang, K., K. Yahya, Y. Zhang, C. Hogrefe, G. Pouliot, C. Knote, R. San Jose and J. L. Perez, P. J. Guerrero, R. Baro, and P. Makar, 2014a, Evaluation of Column Variable Predictions Using Satellite Data over the Continental United States: A Multi-Model Assessment for the 2006 and 2010 Simulations under the Air Quality Model Evaluation International Initiative (AQMEII) Phase 2, *Atmospheric Environment*, this submitted.

Wang, K., K. Yahya, Y. Zhang, S.-Y. Wu, and G. Grell, 2014b, Implementation and Initial Application of A New Chemistry-Aerosol Option in WRF/Chem for Simulation of Secondary Organic Aerosols and Aerosol Indirect Effects, *Atmospheric Environment*, submitted.

Wong, D. C., Pleim, J., Mathur, R., Binkowski, F., Otte, T., Gilliam, R., Pouliot, G., Xiu, A., Young, J. O., and Kang, D., 2012. WRF-CMAQ two-way coupled system with aerosol feedback: software development and preliminary results, Geosci. Model Dev., 5, 299-312, doi:10.5194/gmd-5-299-2012.

Xiu, A. and Pleim, J. E. (2001), Development of a land surface model. Part I: application in a mesoscale meteorological model, J. Appl. Meteorol., 40, 192–209.

Yahya, K., K. Wang, M. Gudoshava, T. Glotfelty, and Y. Zhang, 2014a, Application of WRF/Chem over the continental U.S. under the AQMEII Phase II: Comprehensive Evaluation of 2006 Simulation, *Atmospheric Environment*, in review.

Yahya, K., K. Wang, Y. Zhang, C. Hogrefe and G. Pouliot, and T. E. Kleindienst, 2014b, Application of WRF/Chem over the continental U.S. under the AQMEII Phase II: Comprehensive Evaluation of 2010 Simulation and Responses of Air Quality and Meteorology-Chemistry Interactions to Changes in Emissions and Meteorology from 2006 to 2010, *Atmospheric Environment*, submitted.

867 Yardwood, G., Rao, S., Yocke, M., Whitten, G. Z., 2005. Updates to the Carbon Bond chemical
868 mechanism: CB05. Final Report to the US EPA, RT-0400675, 8 December 2005.

869 Zhang, Y., 2008, Online Coupled Meteorology and Chemistry models: History, Current Status, and
870 Outlook, *Atmos. Chem. and Phys*, 8, 2895-2932.

871

Table 1. Methodologies used in simulating aerosol direct and indirect effects and feedbacks in the suite of models.

Domain	**Model (AQMEII-2 ID) and references**	**Direct Effect Methodology**	**Indirect Effect Methodology and Cloud Microphysics**	**Parameterized Clouds**	**Aerosol Size Representation and processes**	**Meteorological I.C./B.C.**	**Land Surface Model**	**PBL Scheme**	**Radiative Transfer Scheme**	**Gas-Phase Chemical Mechanism**	**Time Period, Data available for comparisons**
NA	GEM-MACH 1.5.1(CA2, CA2f) Moran *et al*, 2010.	Mie scattering: Bohren and Huffman, 1983	Milbrandt and Yao, 2005 (a,b). No-feedback CCN activation: Cohard *et al* , 1998 . Feedback CCN activation: Abdul-Razzak and Ghan, 2002).	Kain and Fritsch (1990) and Kain (2004)	Sectional, 12 bins; Gong *et al*, 2003a,b	15km resolution GEM simulations (Mailhot *et al*., 2006) driven by CMC regional operational analyses (Filion *et al*, 2010)	ISBA2, Belair *et al*., 2003a,b	Moistke4: Mailhot and Benoit, (1982); Belair *et al*. (2005)	Li and Barker (2005)	ADOM-II (Lurmann *et al*., 1986)	2006, 2010, feedback and non-feedback. Both chemical and meteorological variables available for comparisons
	WRF-CHEM 3.4.1 (US8) Grell *et al*., 2005, Skamarock *et al*., 2008, with modifications as described in Wang *et al*, 2014b	Fast-Chapman: *Fast et al*., 2006, *Chapman et al.*, 2009	Chapman *et al*., 2009, Morrison *et al*., 2009. CCN activation: Abdul-Razzak, 2002. No feedback: constant cloud droplet number: 250 cm^{-3}	Grell 3D scheme (Grell and Freitas, 2013)	Modal: MADE3; Ackerman *et al*, 1998; Grell *et al*, 2005	NCEP FNL (1.0°)http://rda.ucar.edu/	NOAH; Chen and Dudhia, 2001; Ek *et al*, 2003	YSU (Hong *et al*., 2006).	RRTMG : Clough et al (2005)	CB-V (Yarwood *et al*, 2005)	2006, 2010 feedback simulations, weather-only simulations. Meteorological variables available for comparisons
	WRF-CMAQ 5.0.1 (US6) Byun and Schere, 2006; Foley *et al*, 2010, Wong *et al*, 2012; Appel *et al*., 2013	CMAQ Feedback: *Bohren and Huffman*, 1998, *Wong et al*.,2012	None; the cloud droplet concentration : 250 cm^{-3}.	KF2 scheme (Kain, 2004)	AERO6 3-modal; Appel *et al*., 2013	NCEP NAM 12-km resolution meteorology; WRF-CHEM: NCEP FNL 1° resolution analyses	Xiu and Pleim,2001	ACM2 (Pleim 2007a,b);	RRTMG : Clough et al (2005)	CB-V-TU (Sarwar *et al*, 2011)	June 1 to September 1, 2006; May 1 to October 1, 2010. Both chemical and meteorological variables available for comparison.
EU	WRF-CHEM 3.4.1 (Feedback: SI1,basecase: SI2) Grell *et al*., 2005, Skamarock *et al*., 2008	Fast-Chapman *Fast et al*., 2006, *Chapman et al*.,2009	None; the cloud droplet concentration : 250 cm^{-3}.	Morrison *et al*. 2009 Grell-3D Grell and Freitas, 2013; Grell and Dévényi, 2002	MADE-SORGAM (Ackermann *et al*., 1998; Schell *et al*., 2001)	ECMWF: 3-hourly data from the ECMWF operational archive (analysis at 00 and 12 UTC and the respective 3/6/9 hour forecasts) with the spatial resolution of 0.25° on 91 model-levels	NOAH (Chen and Dudhia, 2001),	YSU (Hong *et al*., 2006)	Clough *et al*, 2005; Iacono *et al*. 2008	CB-IV-Modified (Sauter *et al*, 2012)	2010, feedback and non-feedback. Both chemistry and meteorological models available for comparison.
	WRF-CHEM 3.4.0 + (New experimental version based on v 3.4; IT2) Grell *et al*., 2005, Skamarock *et al*., 2008	Direct effects simulated following Fast *et al*., 2006, *Chapman et al*. ,2009	Chapman *et al*. (2009),, (Morrison *et al*., 2009), CCN activation: Abdul-Razzak (2002). No feedback: constant cloud droplet number: 250 cm^{-3}		MADE-VBS aerosol scheme (Ahmadov et al., 2012					RACM (Stockwell *et al*, 1997)	2010, feedback and weather-only simulation. Meteorological variables available for comparison.

1 Table 2 Statistical measures used to compare Feedback (F) and No-Feedback (NF) simulations

2

Statistical Measure	**Description**	**Formula**
PCC	Pearson Correlation Coefficient	$PCC = \frac{N\sum_{i=1}^{N}(NF_i \cdot F_i) - \sum_{i=1}^{N}(F_i)\sum_{i=1}^{N}(NF_i)}{\sqrt{N\sum_{i=1}^{N}(F_i \cdot F_i) - \sum_{i=1}^{N}(F_i)\cdot\sum_{i=1}^{N}(F_i)}\sqrt{N\sum_{i=1}^{N}(NF_i \cdot NF_i) - \sum_{i=1}^{N}(NF_i)\cdot\sum_{i=1}^{N}(NF_i)}}$
MD	Mean Difference	$MD = \frac{1}{N}\sum_{i=1}^{N}(F_i - NF_i)$
MAD	Mean Absolute Difference	$MAD = \frac{1}{N}\sum_{i=1}^{N}\lvert F_i - NF_i\rvert$
MSD	Mean Square Difference	$MSD = \frac{1}{N}\sum_{i=1}^{N}(F_i - NF_i)^2$
Intercept	Intercept of observations vs. model best-fit line	$a = \overline{F} - b \cdot \overline{NF}$
NMD	Normalized Mean Difference	$NMD = \frac{\sum_{i=1}^{N}(F_i - NF_i)}{\sum_{i=1}^{N}NF_i} x100$
NMAD	Normalized Mean Absolute Difference	$NMAD = \frac{\sum_{i=1}^{N}\lvert F_i - NF_i\rvert}{\sum_{i=1}^{N}NF_i} x100$
RMSD	Root Mean Square Difference	$RMSD = \sqrt{\frac{1}{N}\sum_{i=1}^{N}(F_i - NF_i)^2}$
Slope	Slope of observations vs. model best-fit line	$b = \frac{\sum_{i=1}^{N}\left[\left(NF_i - \overline{NF}\right)\left(F_i - \overline{F}\right)\right]}{\sum_{i=1}^{N}\left[\left(NF_i - \overline{NF}\right)^2\right]}$

STD	Standard Deviation (Feedback and No-Feedback)	$STD = \frac{\sum_{i=1}^{N}\left(F_i - \overline{F}_i\right)^2}{N}, \frac{\sum_{i=1}^{N}\left(NF_i - \overline{NF}_i\right)^2}{N}$
DSTD	Change in standard deviation (used to compare two model's variability, where F and NF are the Feedback and No-Feedback models, respectively)	$DSTD = \frac{\sum_{i=1}^{N}\left(F_i - \overline{F}_i\right)^2}{N} - \frac{\sum_{i=1}^{N}\left(NF_i - \overline{NF}_i\right)^2}{N}$

Table 3. Minimum hourly grid correlation coefficients feedback versus no-feedback simulations

Variable	NA lowest correlation coefficient	EU lowest correlation coefficient
Surface temperature	0.885	0.974
Downward shortwave at the surface	0.30	0.65
Upward shortwave at the surface	0.52	0.61
Upward shortwave at the model top	0.10	0.60
PBL Height	0.20 (most >0.60)	0.75
Precipitation	0.00	0.25
Cloud Liquid Water Path	0.06	0.30

Table 4. Summary of feedback impacts, by variable, model and domain

Variable	Model	Direct (D), Direct + Indirect (I+D) Feedbacks implemented	Domain	Impact
Temperature	GEM-MACH	D+I	NA	Winter increases, summer decreases
	WRF-CHEM			
	WRF-CHEM	D+I	EU	Summer increases, winter decreases
	WRF-CHEM	D	EU	Decreases
	WRF-CMAQ		NA	
Surface Downward Shortwave	GEM-MACH	D+I	NA	Increases/decreases
	WRF-CHEM		EU	
	WRF-CHEM		NA	Decreases
	WRF-CMAQ	D	NA	Decreases
	WRF-CHEM		EU	
Surface Upward Shortwave	GEM-MACH	D+I	NA	Increases/decreases
	WRF-CHEM			
	WRF-CHEM		EU	
	WRF-CMAQ	D	NA	Decreases
	WRF-CHEM		EU	
Top Upward Shortwave	GEM-MACH	D+I	NA	Dominantly increases
	WRF-CHEM			
	WRF-CMAQ	D		
	WRF-CHEM	D	EU	
	WRF-CHEM	D+I	EU	Dominantly decreases
Precipitation	WRF-CHEM	D	EU	Dominantly decreases
	WRF-CMAQ		NA	
	GEM-MACH	D+I	NA	Dominantly increases
	WRF-CHEM		EU	
	WRF-CHEM		NA	Increases and decreases
Cloud Liquid Water Path	GEM-MACH	D+I	NA	Increases
	WRF-CHEM		EU	Decreases
PBL height	GEM-MACH	D+I	NA	Summer decreases, winter increases
	WRF-CHEM			
	WRF-CHEM	D+I	EU	Decreases
	WRF-CMAQ	D	NA	Decreases
	WRF-CHEM		EU	

Table 5. Summary of Comparisons to Observations, NA (after Brunner et al, 2014). Italics indicate best score, bold face best score between feedback and no-feedback models. Numbers in brackets refer to biases within subdomains (NA1/NA2/NA3: western, south-eastern, and north-eastern NA), other numbers are averages for the continent

Variable	Bias, NA Models			
	GEM-MACH 1.5.1 (no-feedback)	GEM-MACH 1.5.1 (direct + indirect effect feedback)	WRF-CMAQ 5.0.1 (direct effect feedback)	WRF-CHEM 3.4.1 (direct + indirect effect feedback)
Annual Surface Pressure (mb)	-5.1	***-5.0***	-7.6	-9.0
Annual 2m Temperature (K)	-0.54 (-1.7/-0.7/*0.0*)	**-0.47** (***-1.6/-0.6****/0.0*)	*0.10* (*-0.4/0.1/*-0.1*)*	0.89 (-1.3/-0.8/-1.3)
Precip (cm)	(-0.84/-1.61/-2.91)	(**-0.73/-1.28/-2.03**)	(0.10/0.24/-0.21)	*(0.09/-0.02/-0.19)*
Annual 10 m wind speed (ms^{-1})	(***0.03***/**0.76**/**0.64**)	(0.06/0.78/0.67)	(1.22/*0.53*/0.92)	(0.24/-0.69/*0.01*)

Table 6. Summary of Comparisons to Observations, EU (after Brunner et al, 2014). Italics indicate best score, bold face best score between directly comparable feedback and no-feedback models. Numbers in brackets refer to biases within subdomains (EU1/EU2/EU3: north-western Europe, north-eastern Europe and southern Europe and Turkey). Other numbers are averages for the continent.

Variable	BIAS, EU Models		
	WRF-CHEM 3.4.1 (no-feedback)	WRF-CHEM 3.4.1 (direct effect feedback)	WRF-CHEM 3.4.0 (direct + indirect effect feedback)
Annual 2m daily mean Temperature (K)	(-0.5/-0.8/-0.9)	(-0.5, **-0.7, -0.8**)	(*-0.1/-0.4/-0.5*)
Annual 10 m daily mean wind speed (ms^{-1})	*(1.0/1.3/1.2)*	*(1.0/1.3/1.2)*	(1.4/1.7/1.5)

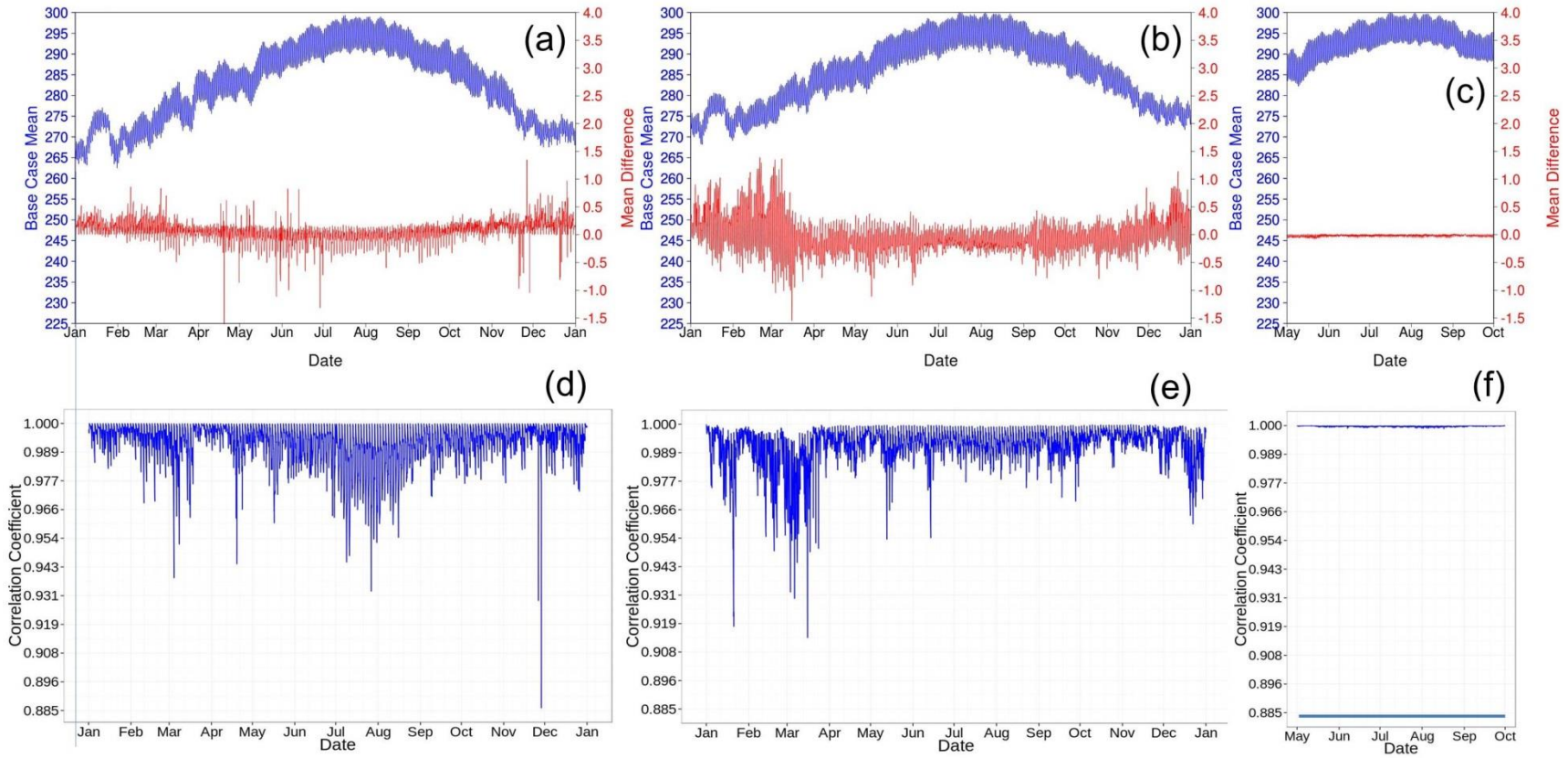

Figure 1. Comparison of hourly grid-mean temperatures, NA domain, 2010 (K). Upper row: non-feedback mean temperature (blue), mean difference (feedback – no-feedback) for (a) GEM-MACH (direct + indirect effect), (b) WRF-CHEM (direct + indirect effect), and (c) WRF-CMAQ (direct effect only). Lower row: spatial correlation coefficient in temperature at each simulated hour for (d) GEM-MACH, (e) WRF-CHEM, and (f) WRF-CMAQ.

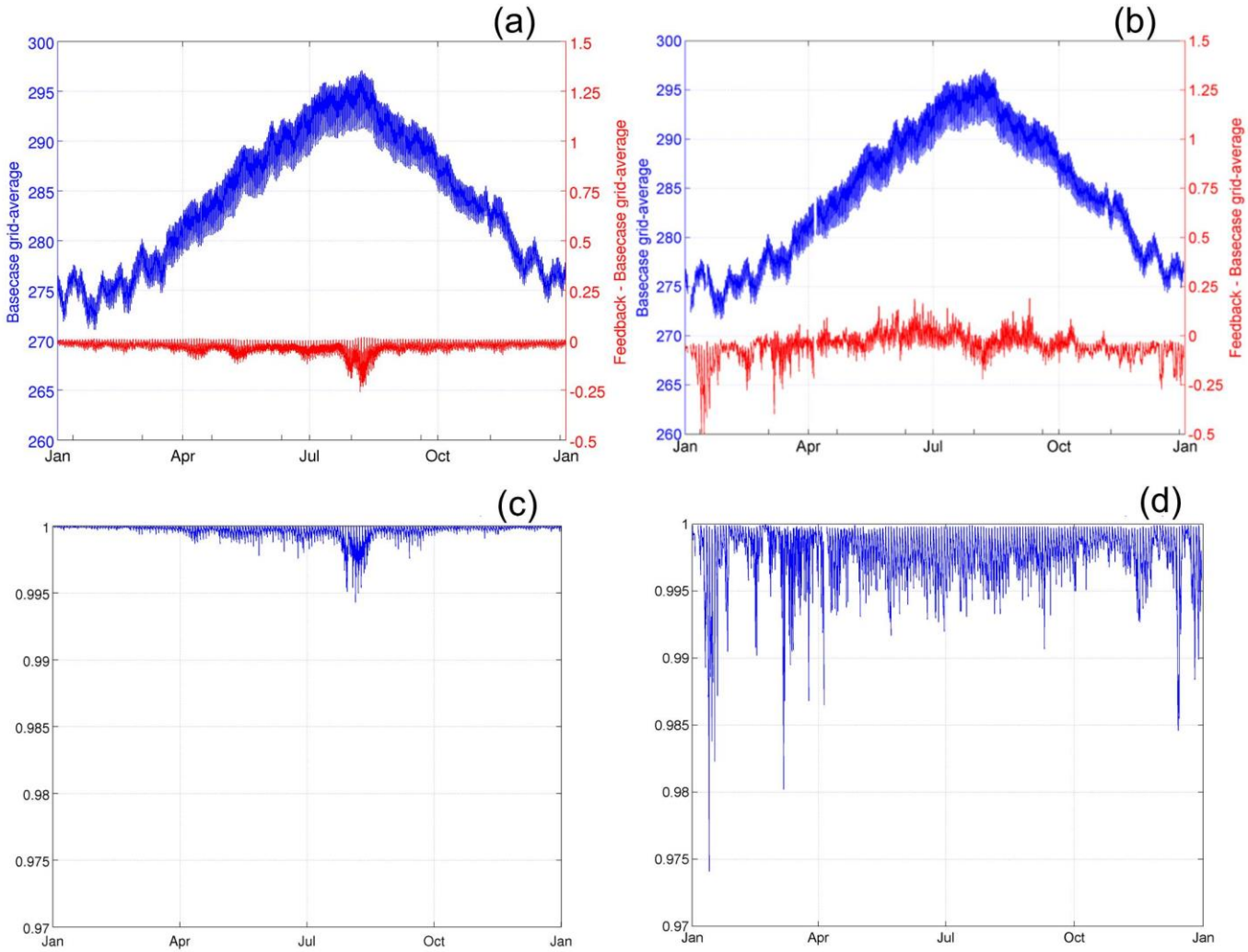

Figure 2. Surface temperature feedback versus no-feedback comparisons for the EU domain, 2010 (K). (a,b): Hourly mean no-feedback temperature and mean temperature difference (Feedback – No-Feedback) for (a) WRF-CHEM 5.4.1 (aerosol direct effect only), WRF-CHEM 5.4.0 (direct + indirect effect). (c,d): Hourly correlation coefficient between Feedback and No-Feedback models for aerosol direct effect (c) and aerosol direct + indirect effect (d).

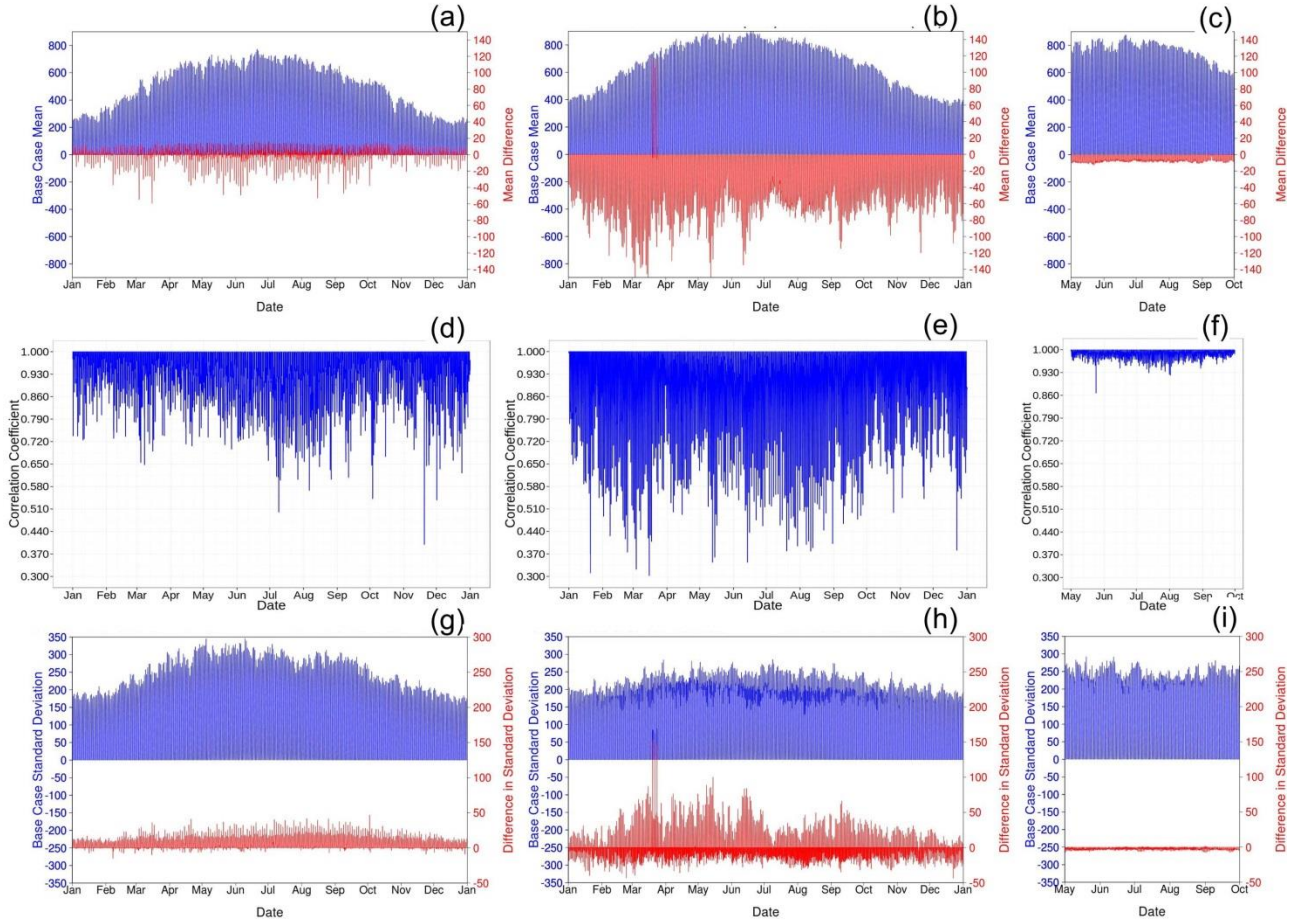

Figure 3. Comparison of hourly grid-mean downward shortwave radiation at the surface for the NA domain, 2010 (W m^{-2}). Columns from left to right are GEM-MACH (direct + indirect effect), WRF-CHEM (direct + indirect effect) and WRF-CMAQ (direct effect only). Rows from top to bottom are non-feedback mean & mean difference, correlation coefficient, and non-feedback standard deviation and difference in standard deviation (feedback – basecase).

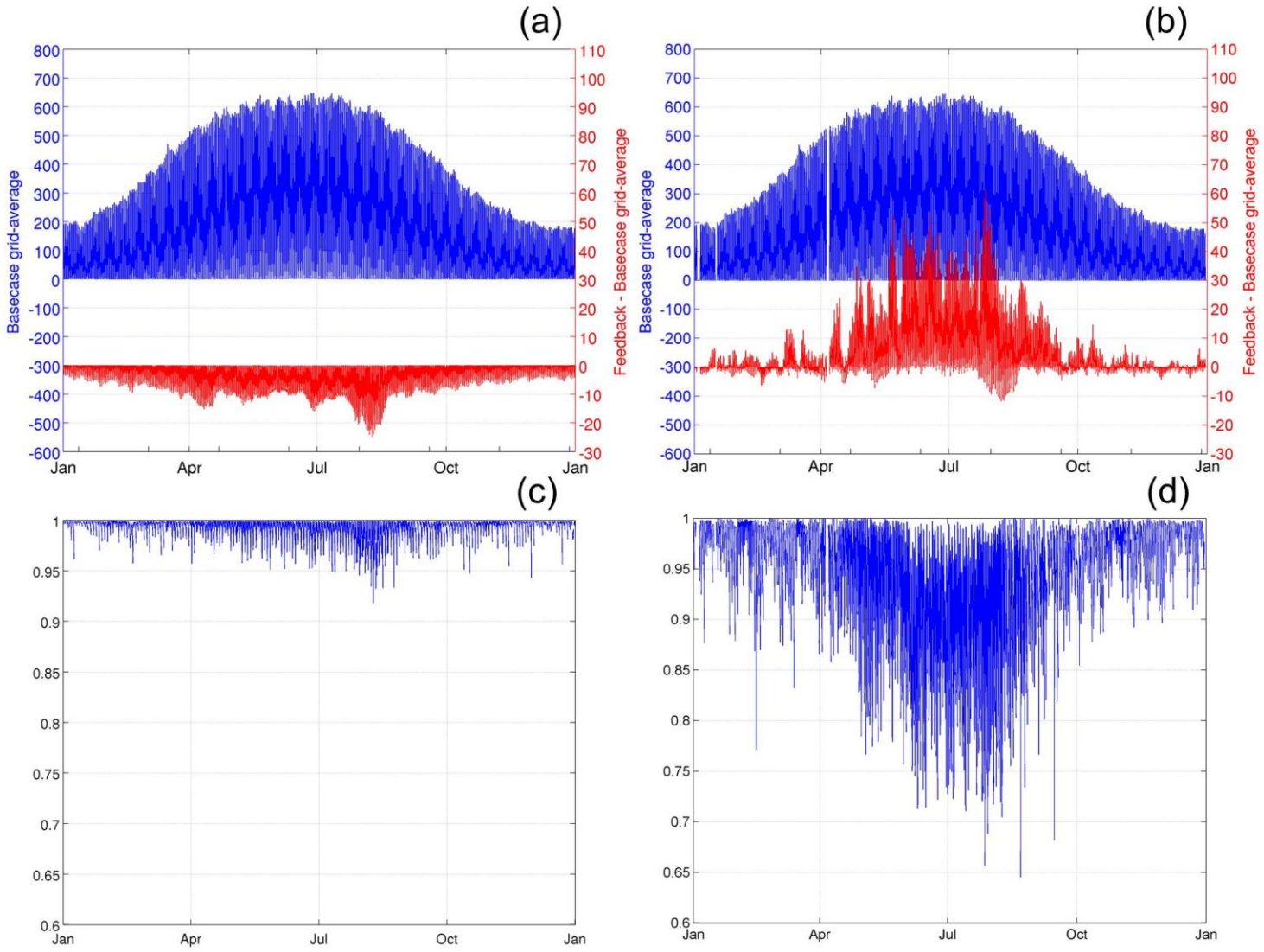

Figure 4. Surface downward shortwave flux feedback versus no-feedback comparisons for the EU domain, 2010 (W m^{-2}). Panels arranged as in Figure 2.

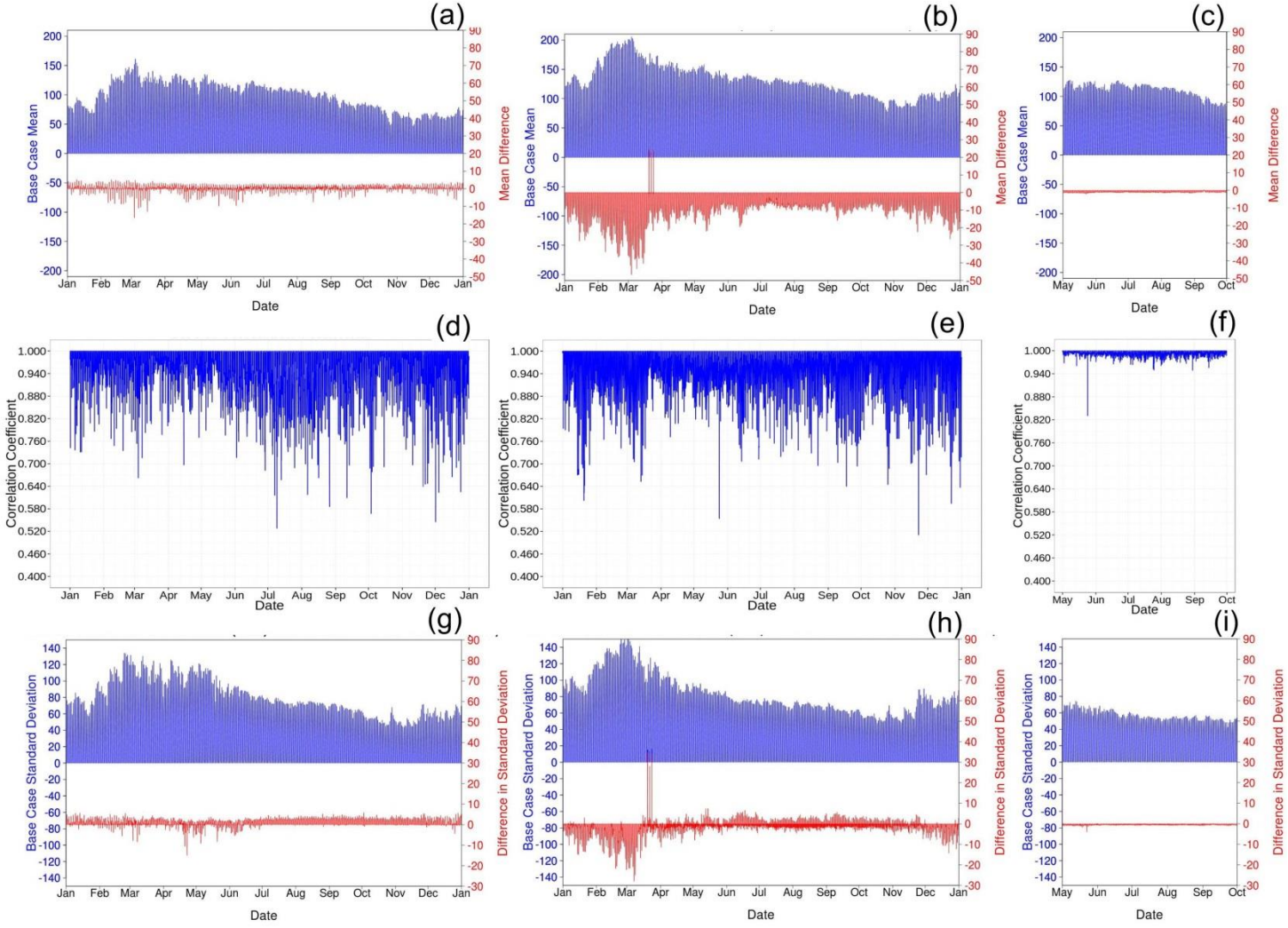

Figure 5. As for Figure 3, for hourly grid-mean upward flux of shortwave radiation at the surface (W m^{-2}).

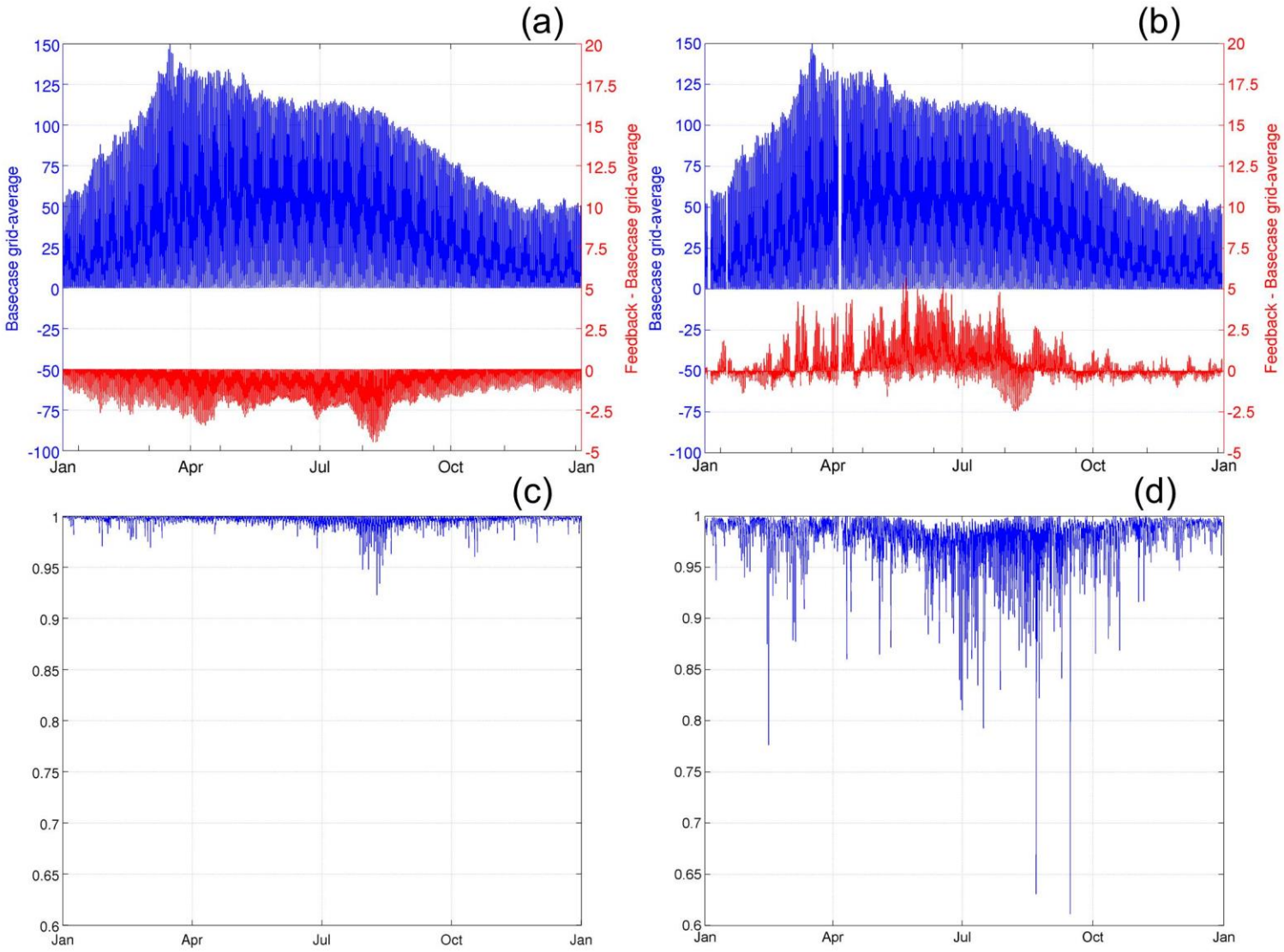

Figure 6. Surface upward shortwave flux feedback versus no-feedback comparisons for the EU domain, 2010 (W m^{-2}). Panels arranged as in Figure 2.

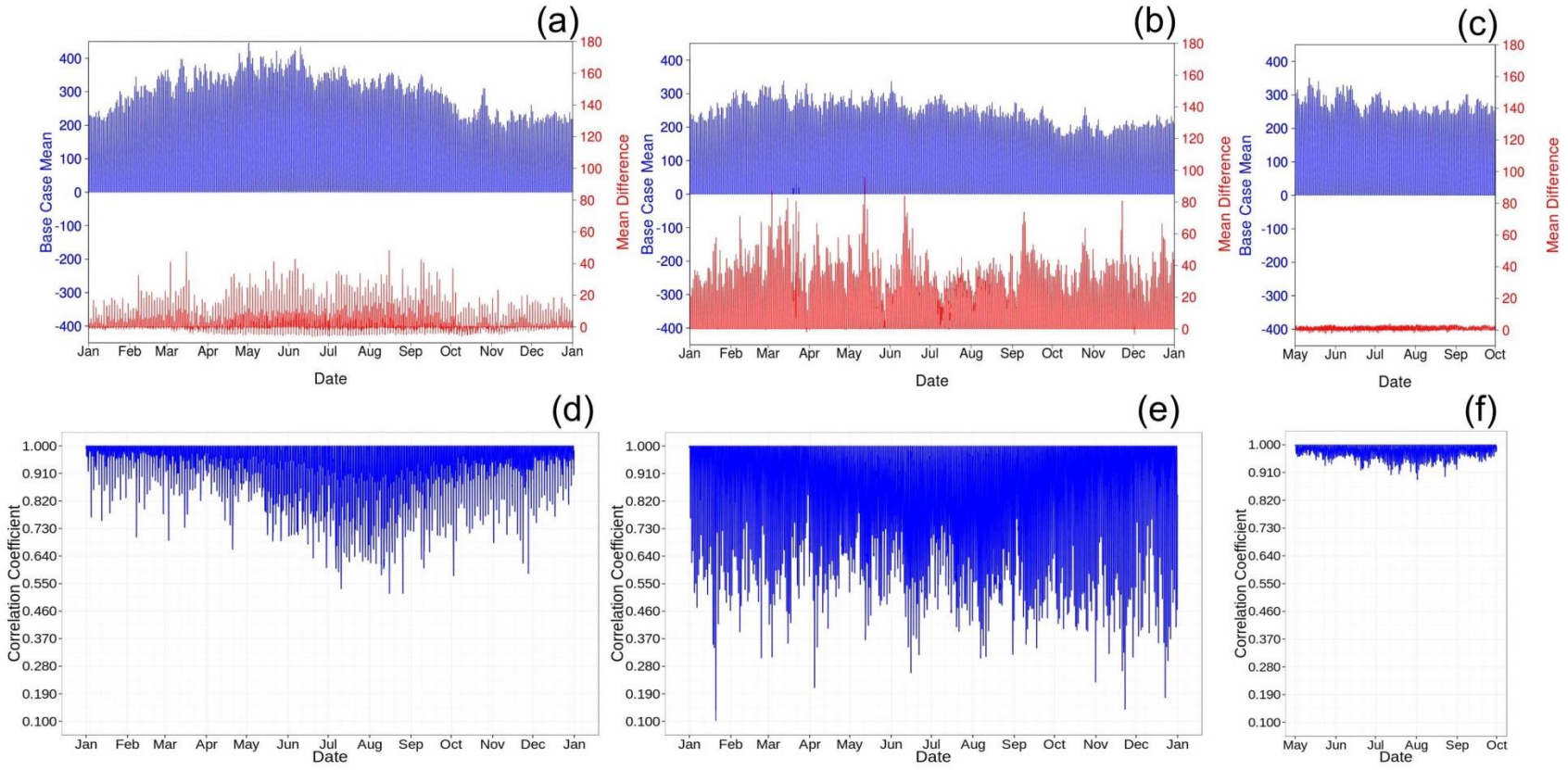

Figure 7. As for Figure 1, for hourly grid-mean upward shortwave radiation at the model top (W m^{-2}).

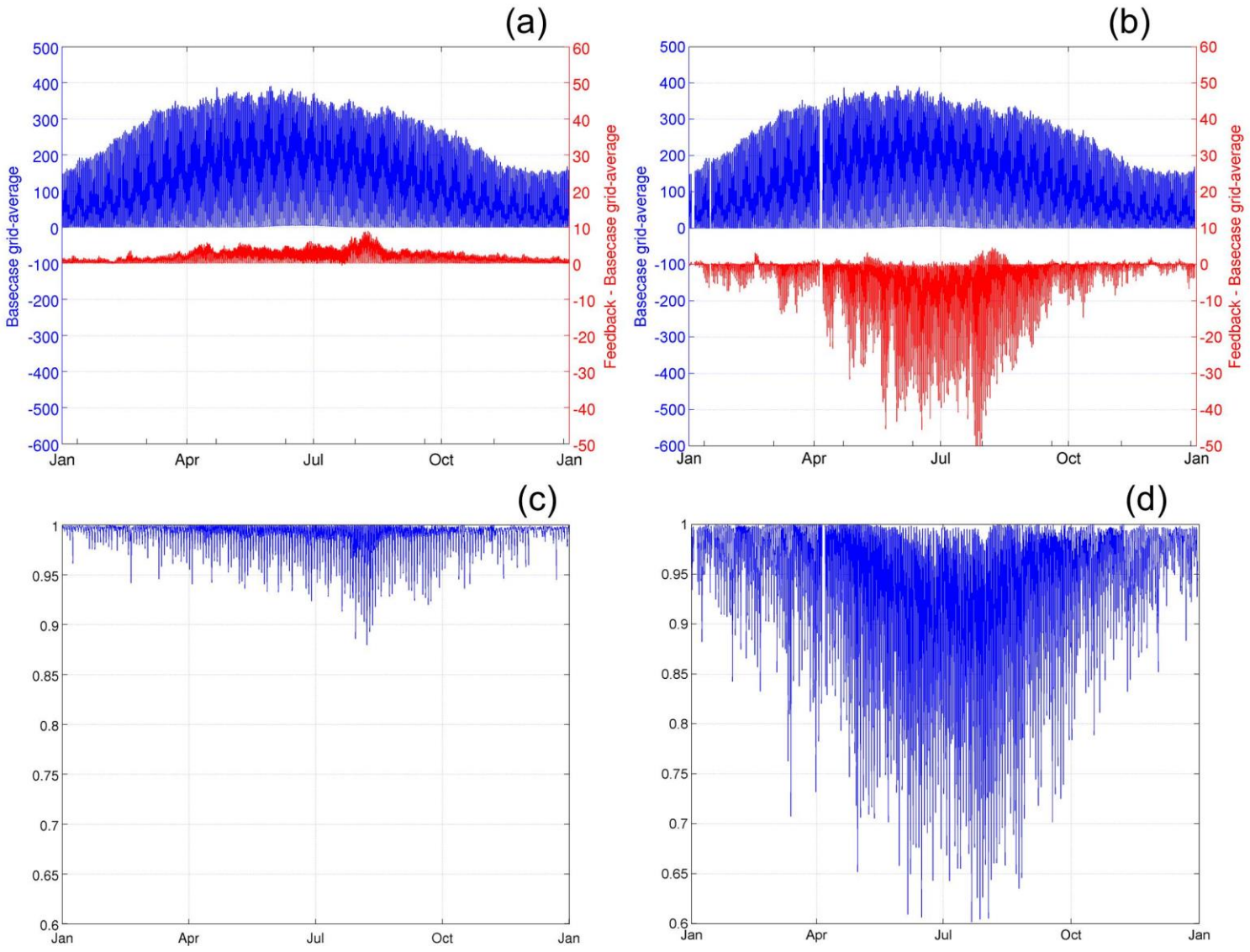

Figure 8. Top-of-model upward shortwave flux feedback versus no-feedback comparisons for the EU domain, 2010 (W m^{-2}). Panels arranged as in Figure 2.

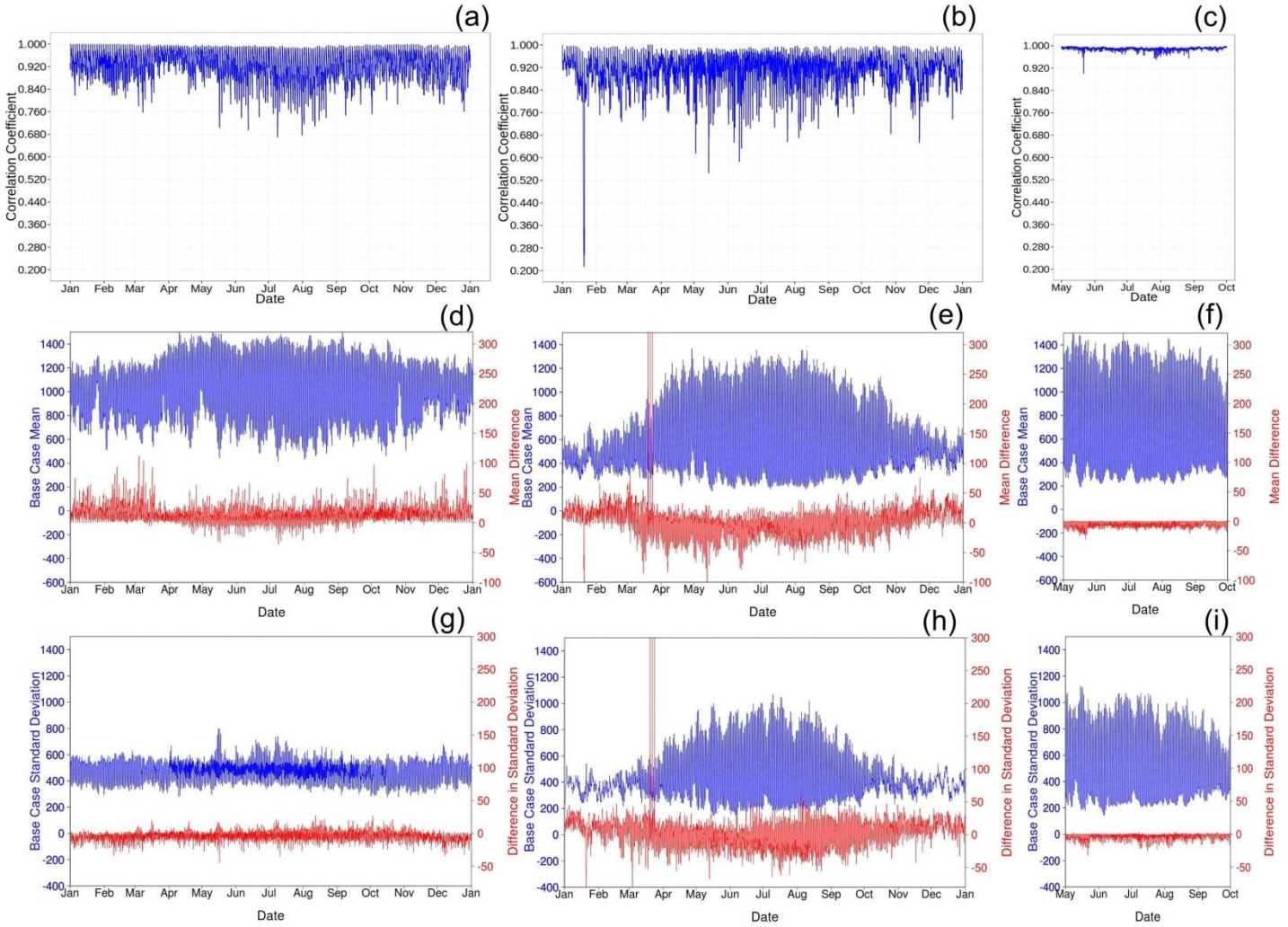

Figure 9. Comparison of hourly grid-mean PBL height, NA domain, 2010 (m). are GEM-MACH (direct + indirect effect), WRF-CHEM (direct + indirect effect) and WRF-CMAQ (direct effect only). Rows from top to bottom are correlation coefficient, non-feedback mean & mean difference, and non-feedback standard deviation and difference in standard deviation (feedback – basecase).

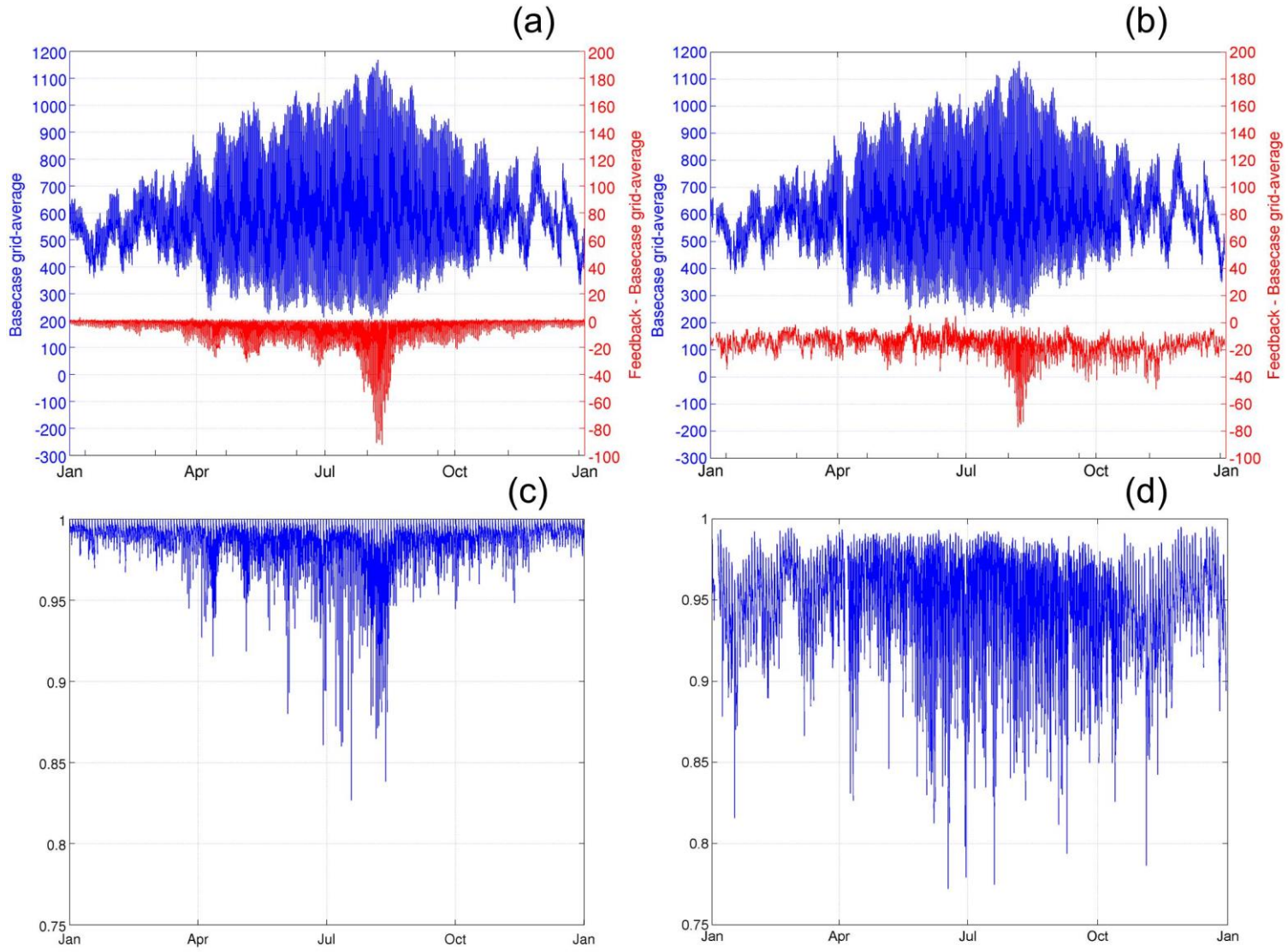

Figure 10. Planetary Boundary Layer Height feedback versus no-feedback comparisons for the EU domain, 2010 (m). Panels arranged as in Figure 2.

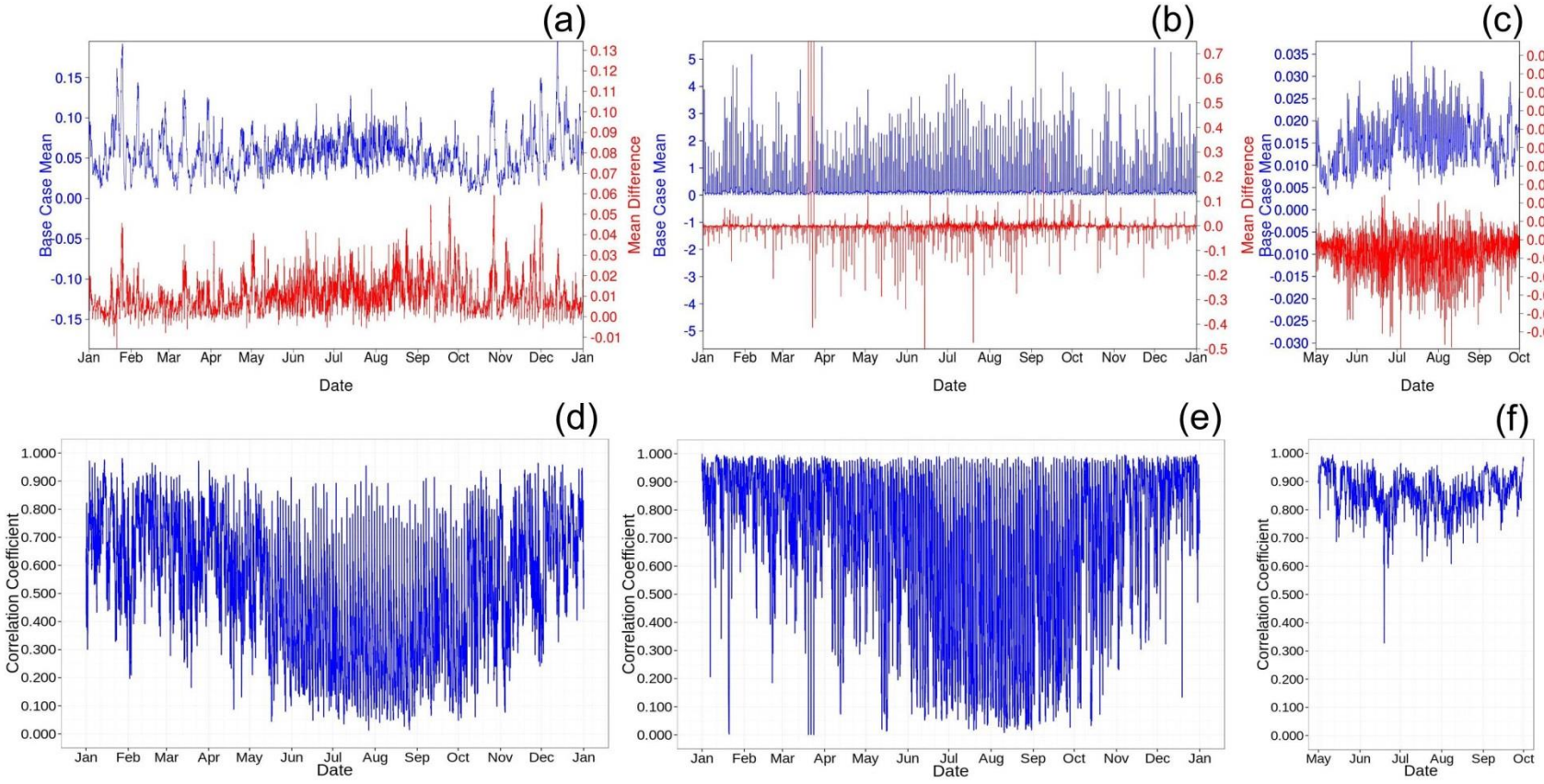

Figure 11. As for Figure 1, Precipitation (grid average mm h^{-1}). Note changes in y-axis scales between (a,b,c).

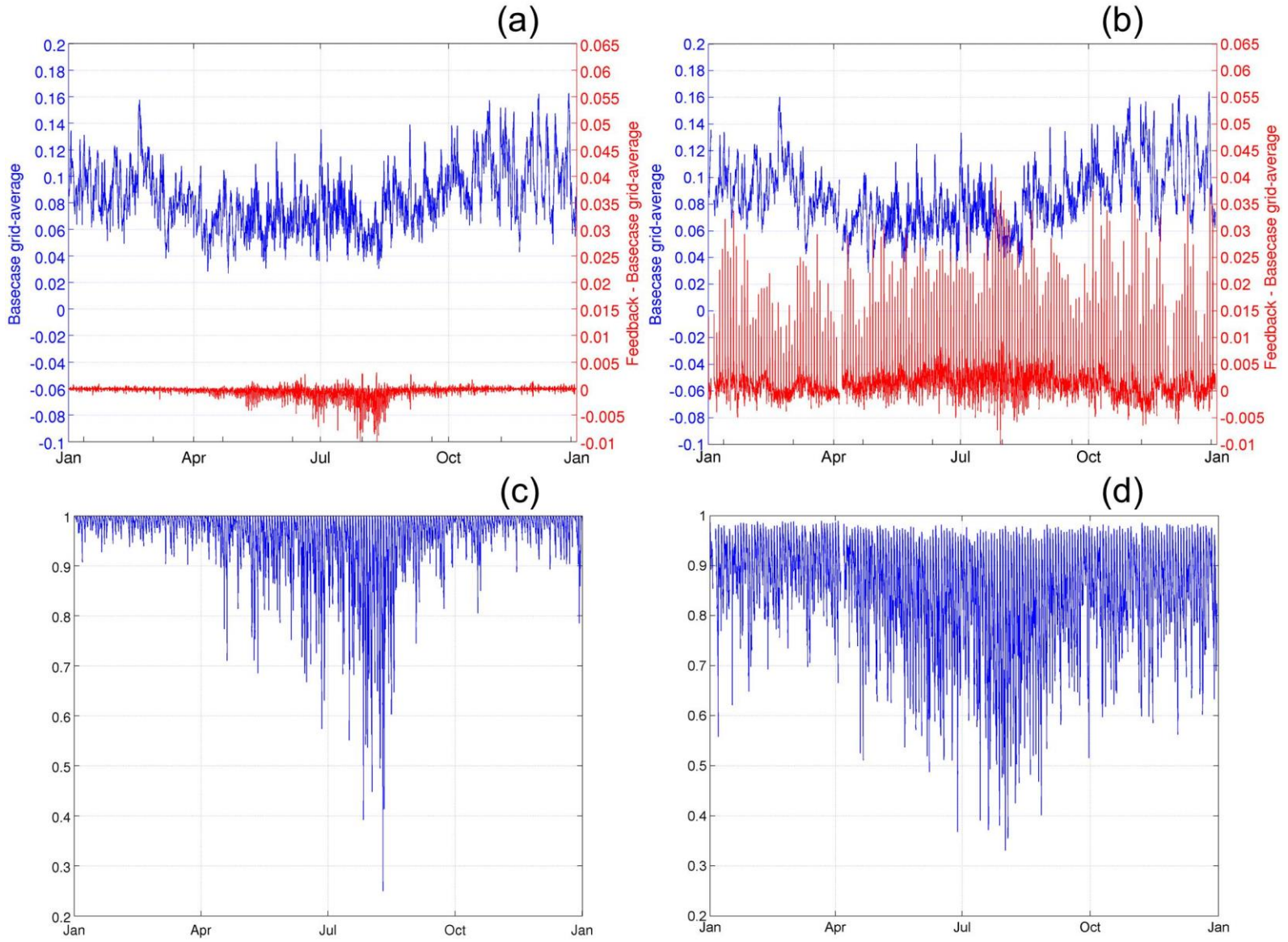

Figure 12. Hourly precipitation, feedback versus no-feedback, EU domain, 2010 (grid average mm h^{-1}). Panels arranged as in Figure 2.

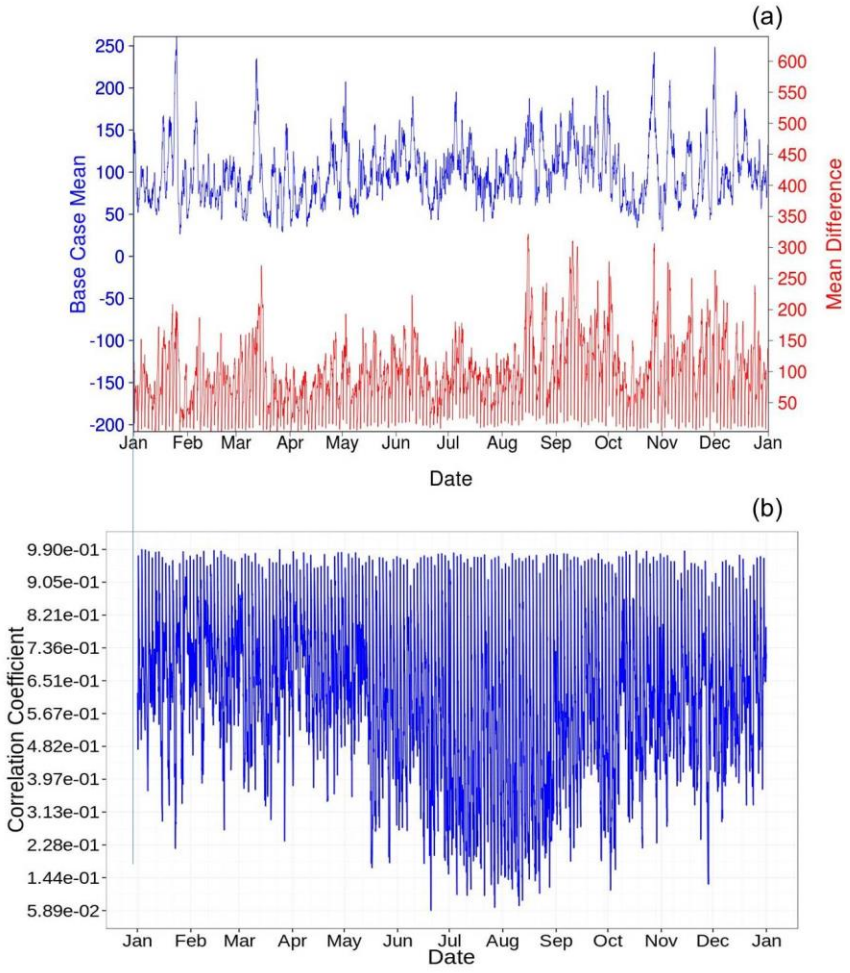

Figure 13. Grid-average cloud liquid water path, GEM-MACH (direct + indirect effect) (g m^{-2}). (a) Mean non-feedback values (blue) and mean difference (feedback – basecase), (b) Correlation coefficient.

81

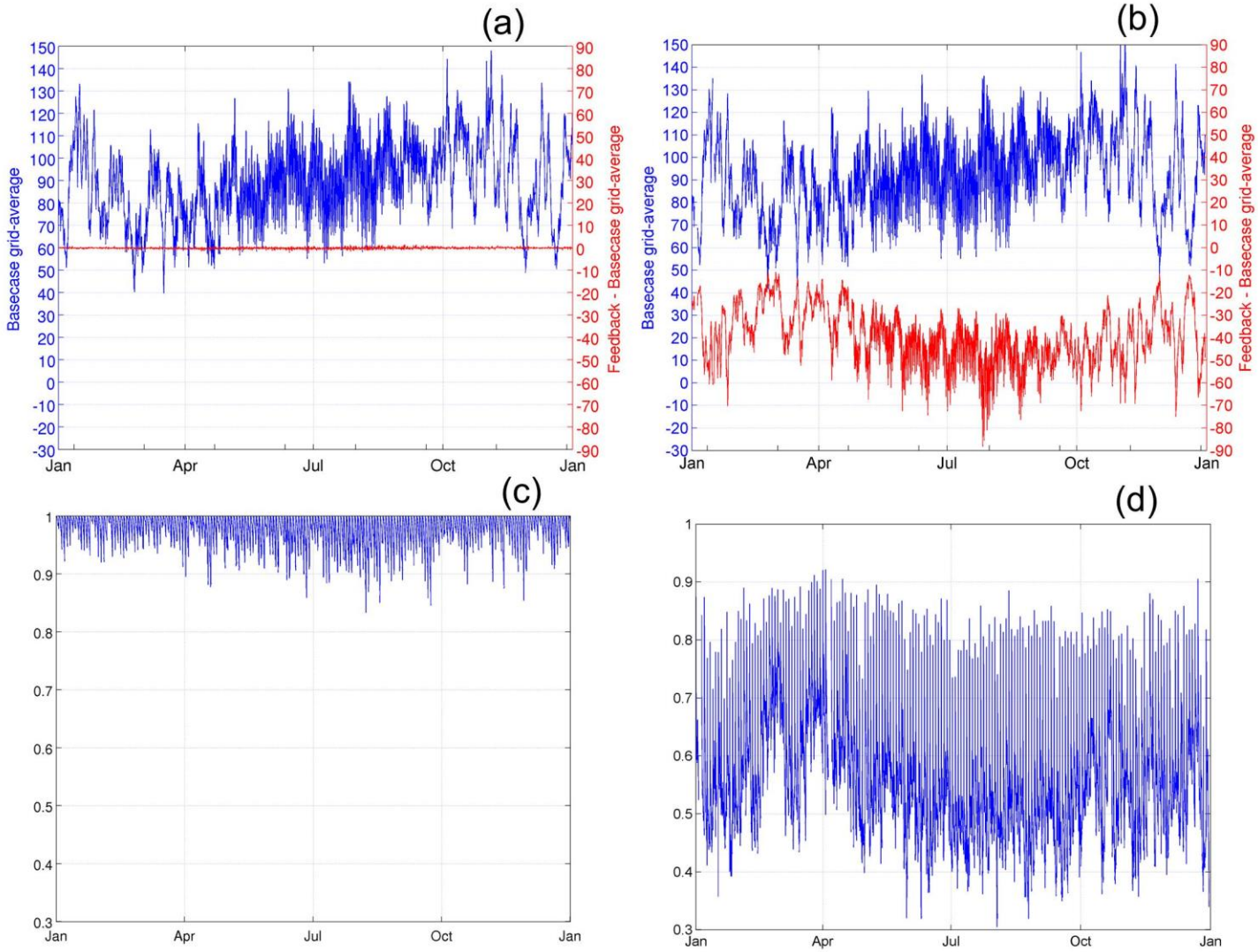

82

83 Figure 14. Hourly Cloud Liquid Water Path, feedback versus no-feedback, EU domain, 2010 (g m^{-2}). Panels arranged as in Figure 2.

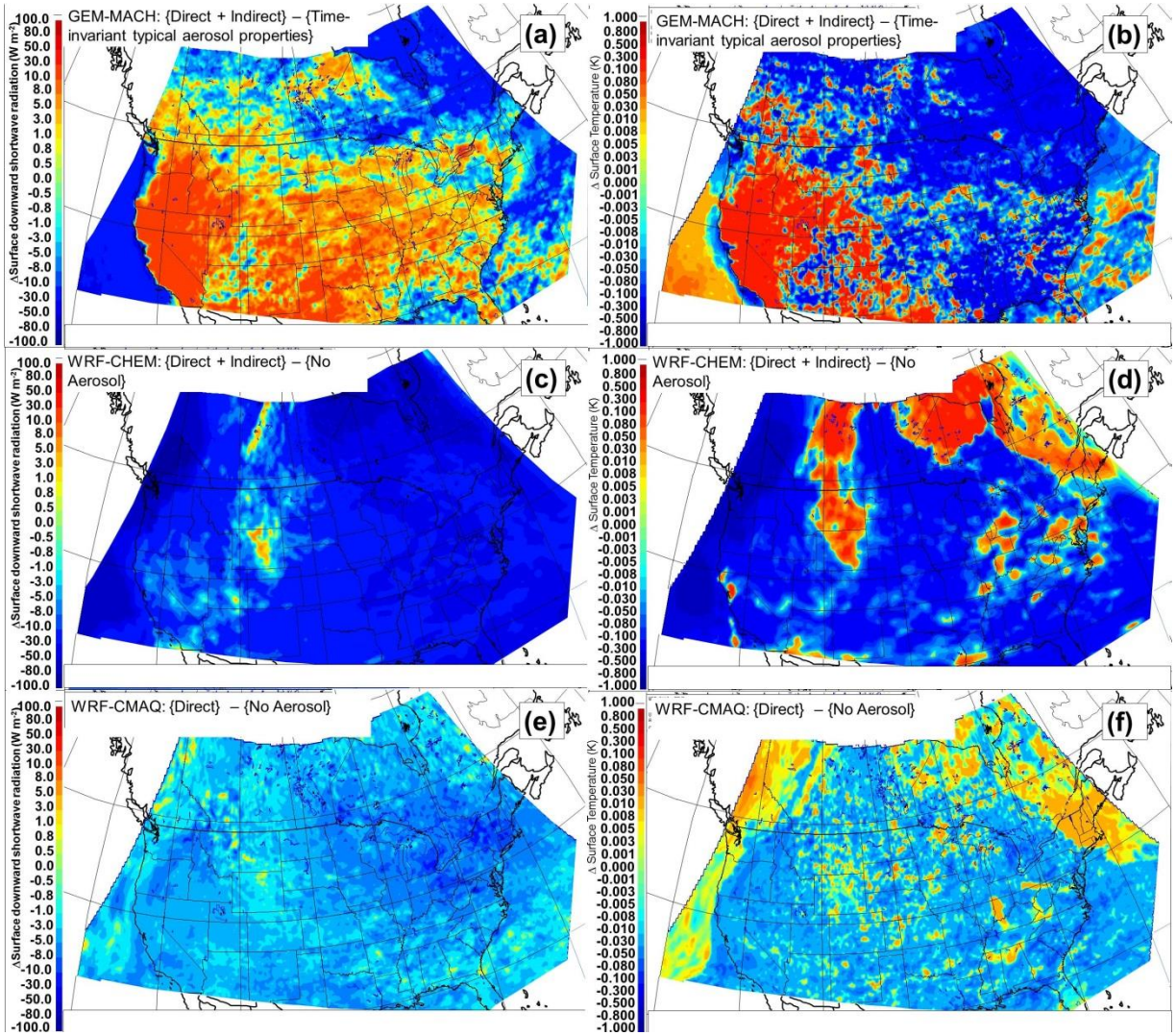

Figure 15. Mean differences for the NA domain, summer analysis period, downward shortwave radiation at the surface (a,c,e) (W m^{-2}) and surface temperature (b,d,f) (K) for GEM-MACH (a,b), WRF-CHEM (c,d), and WRF-CMAQ (e,f).

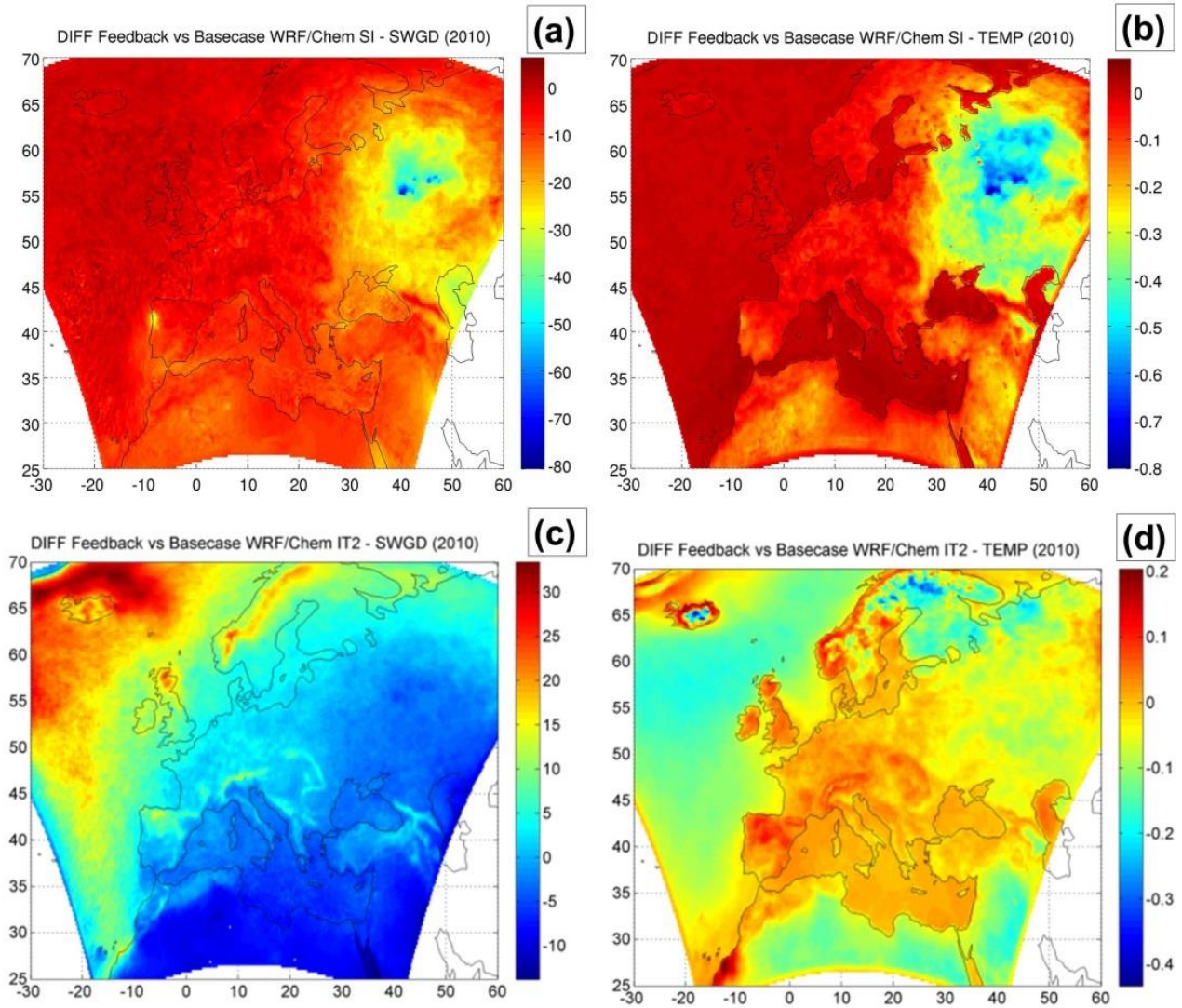

88

89 Figure 16. Comparison of feedback-induced changes in simulated mean hourly downward shortwave radiation (a,c) (W m^{-2}), and surface
90 temperatures (b,d) (K), July 25th to August 19th, EU domain. (a,b): Direct effect only WRF-CHEM. (c,d): Direct + Indirect effect WRF-CHEM.
91 Note changes in colour scale between panels.

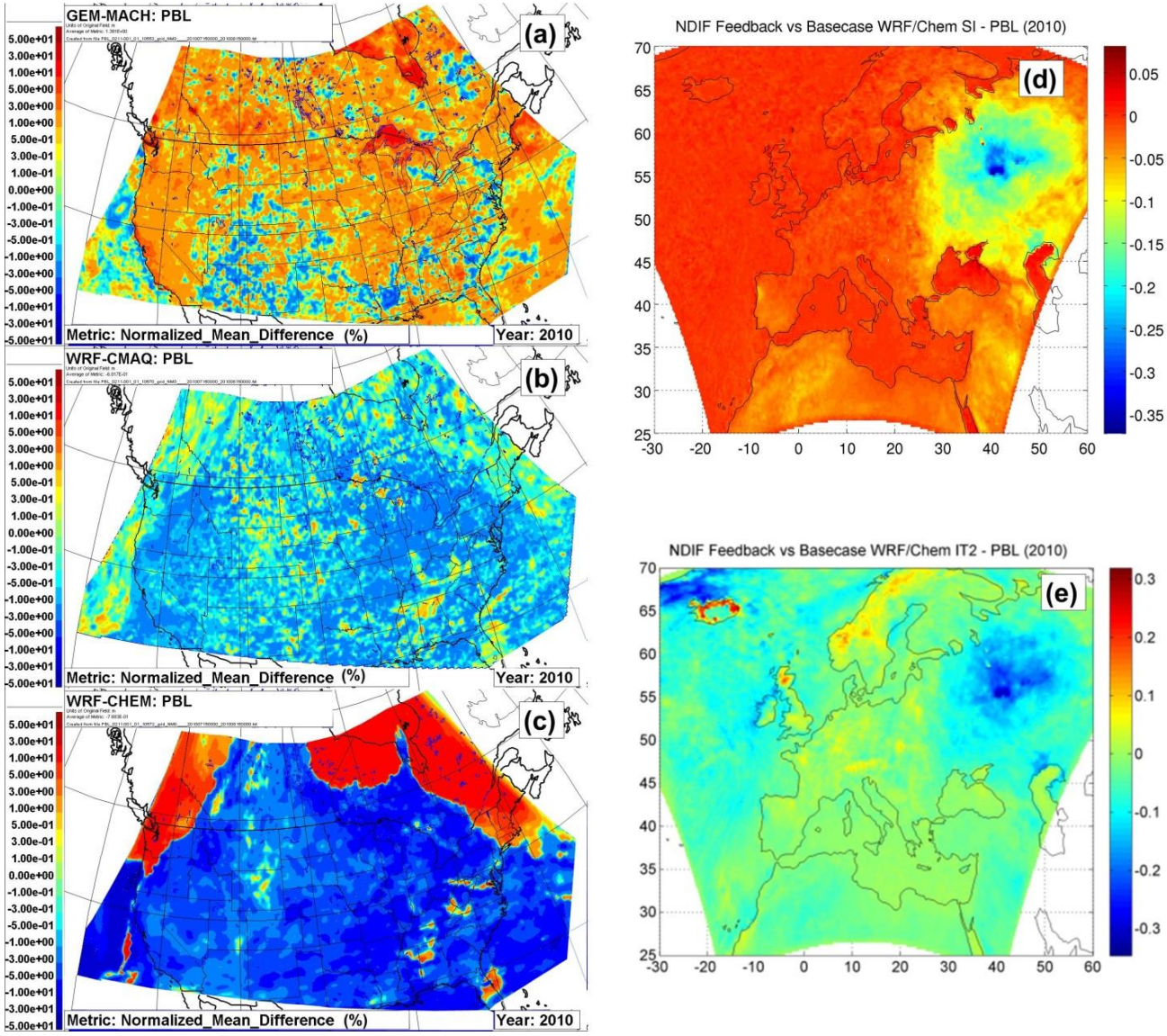

Figure 17. Comparison of feedback-induced changes in simulated PBL height (m) for NA (July 15th to August 15th, a,b,c), and EU (d,e).

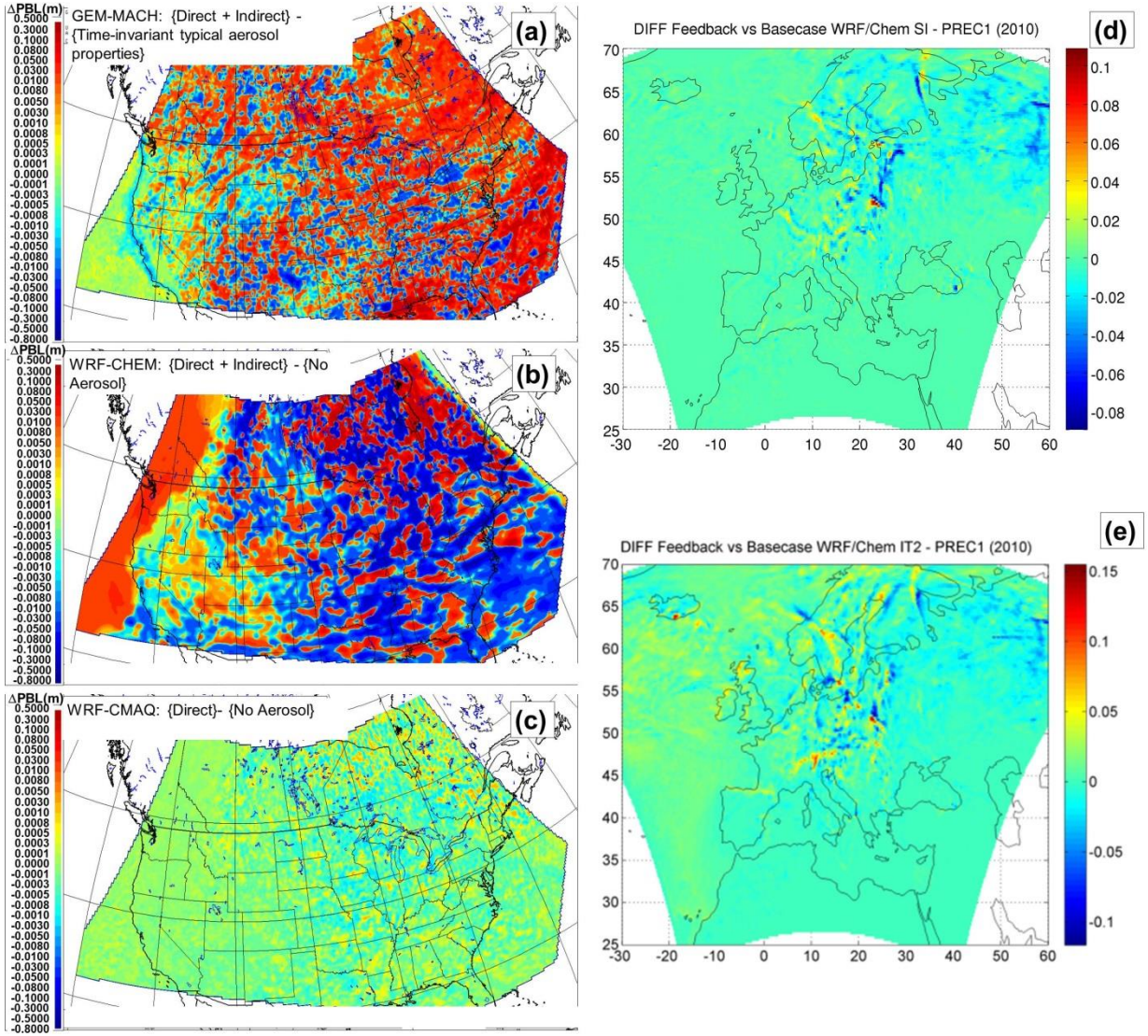

Figure 18. Comparison of feedback-induced changes in simulated average hourly total precipitation for NA (July 15th to August 15th, a,b,c), and EU (July 25th through August 19th, (d,e) (mm h^{-1}).

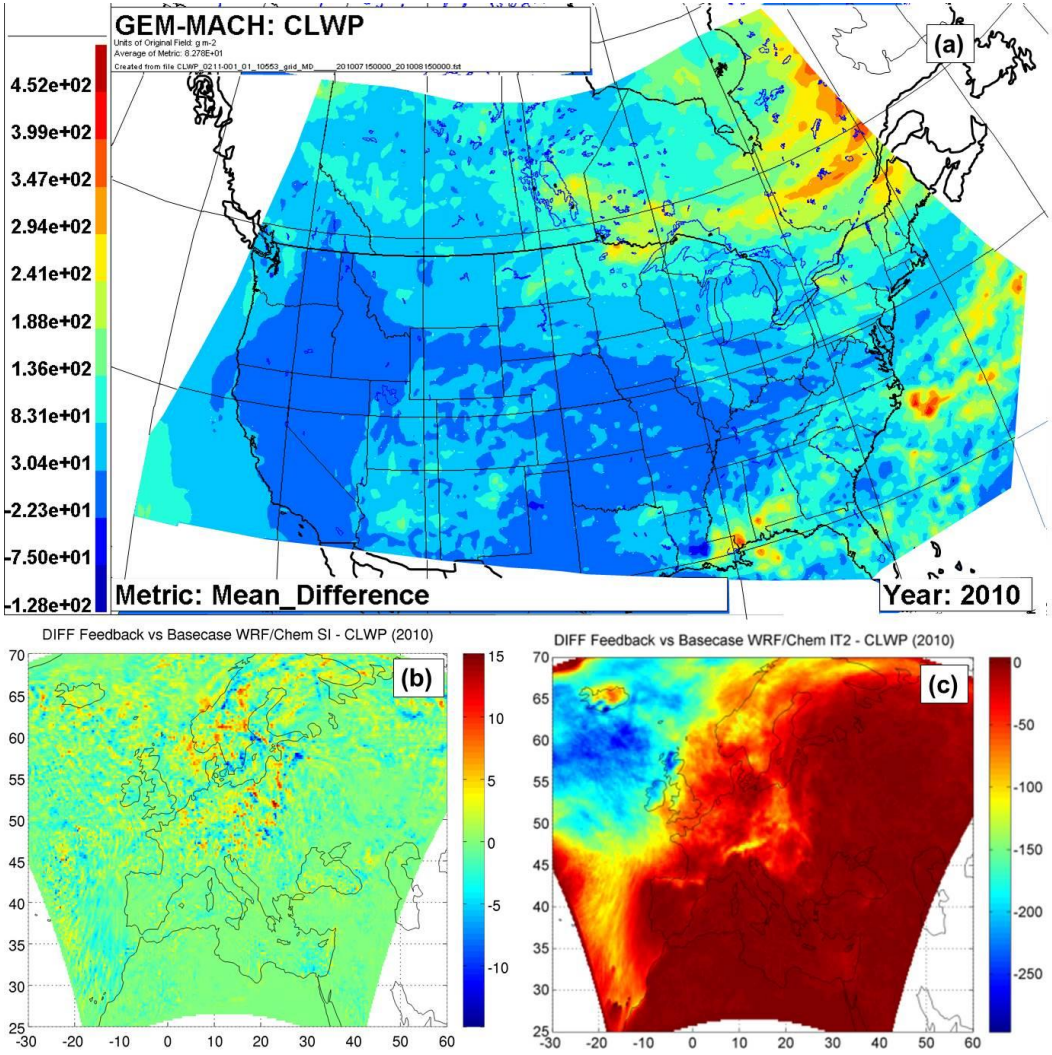

Figure 19. Comparison of summer feedback-induced changes in simulated cloud liquid water path (g m^{-2}) for NA (GEM-MACH, (a)), and EU WRF-CHEM with direct effect (b) and direct + indirect effect (c). Note change in colour scales between panels.

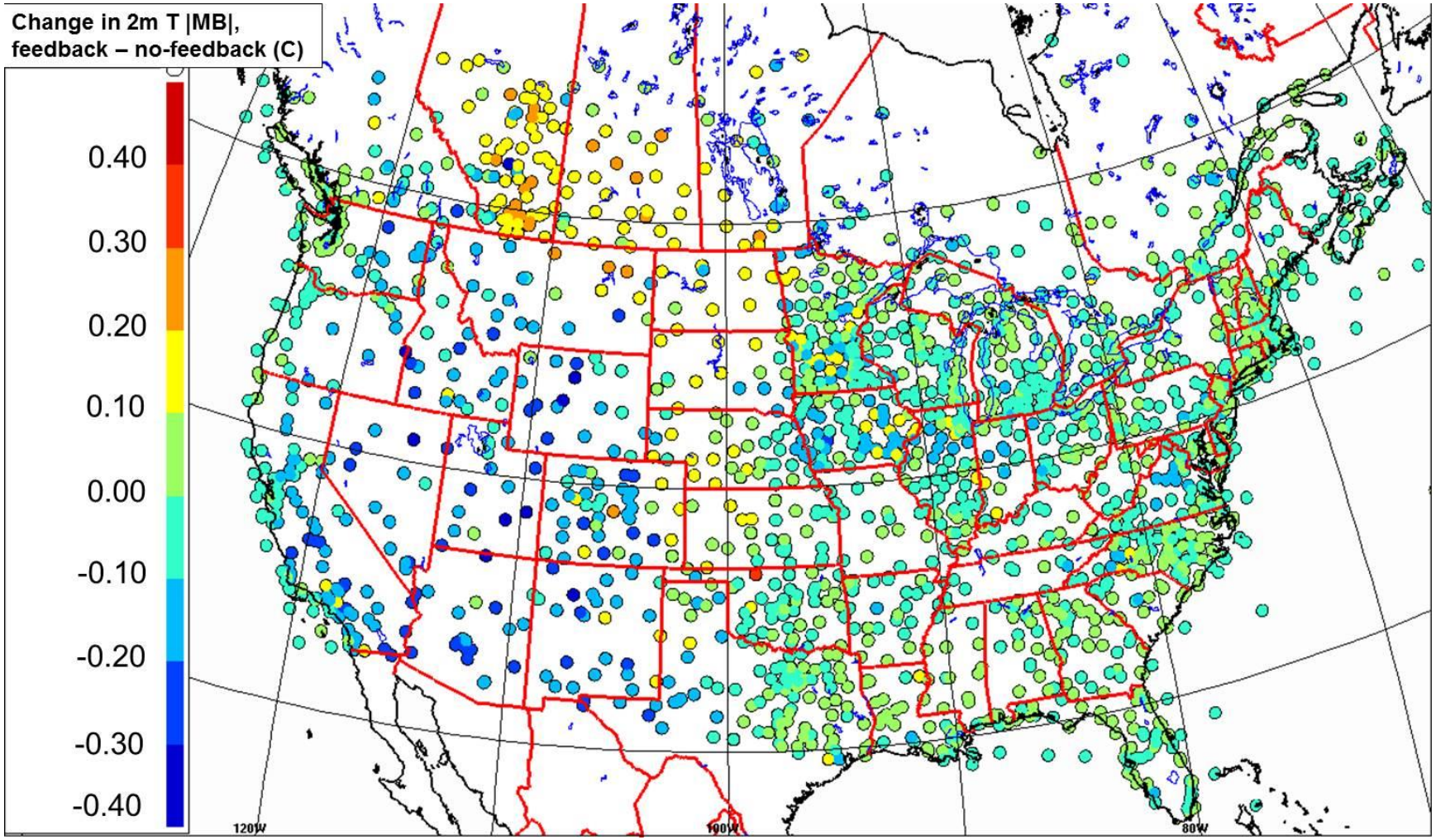

Figure 20. Change in magnitude of annual surface temperature mean bias (K) for GEM-MACH simulation (feedback |MB| - no-feedback |MB|), North American observation sites.

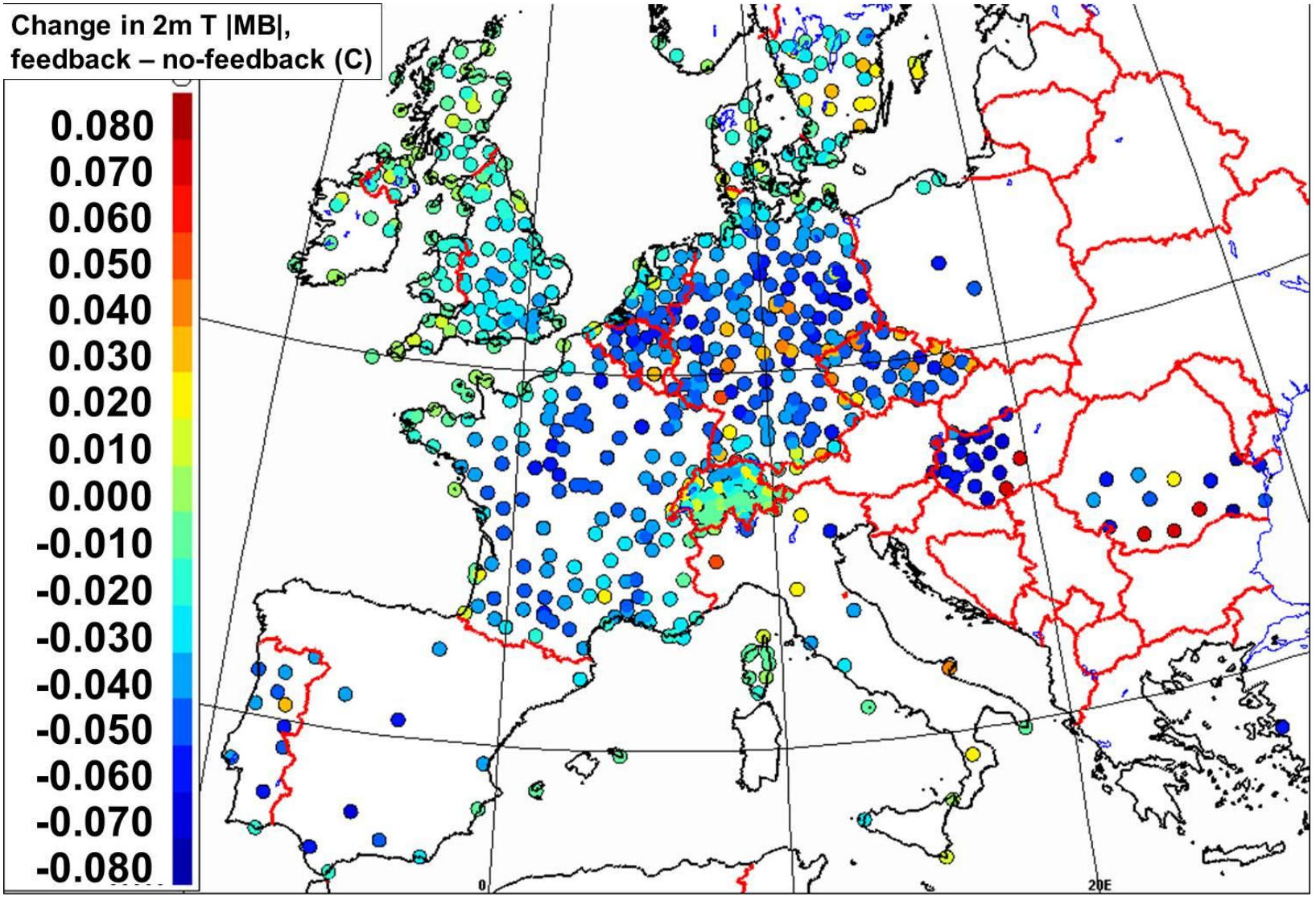

Figure 21. Change in magnitude of annual surface temperature mean bias (K) for WRF-CHEM simulation (feedback |MB| - no-feedback |MB|), European observation sites.